

POLITECNICO DI TORINO

Master Degree in Mechanical Engineering



Thesis

**Experimental and numerical
investigations of MD-based passive and
active desalination technologies**

Academic Supervisor:

Matteo FASANO

Research Advisors:

Matteo MORCIANO

Eliodoro CHIAVAZZO

Candidate:

Nicholas ROTH 265978

ACADEMIC YEAR 2019-2020

*A mia madre
fonte inesauribile di saggezza e forza.*

Abstract

The progressive increase in environmental pollution and population are leading many countries to deal with severe water scarcity issues. Nowadays, it is estimated that at least four billion people live in a water stress condition, and despite the lack of information, there are already many alarming situations.

Water desalination seems to be a promising procedure to mitigate this problem, thanks to several proposals of different technologies. A possible subdivision is in active and passive technologies, where in the former external mechanical components drive the desalination process, while in the latter external mechanical parts are not present. Furthermore, both technologies necessitate of external energy to drive the desalination process, which can be provided by renewable sources. The main goal of this thesis is to analyse an active plant and a passive device, both based on Membrane Distillation, and to compare the two technologies, figuring out the most suitable applications. The first is a Direct Contact Membrane Distillation (DCMD) process-based plant, powered by solar collectors and including a heat storage tank, whose performances are investigated by means of Simulink software. The second is a passive solar driven multi-stage device, capable of recovering the latent heat of the process, developed at the Politecnico di Torino.

The work is subdivided in different sections. In the introduction, the state-of-art of the most important desalination technologies is discussed. Then, the active configuration of the membrane distillation-based technology is studied. In detail, all the parts of the active plant model are described, including the physics behind the process and the software's language used. In addition, the passive configuration of the membrane distillation-based technology is introduced. The design and the prototyping of the device are discussed, with attention in describing the chosen guidelines which are imposed by the worldwide OHDC (Oman Humanitarian Desalination Challenge), used as reference for the device development. In particular, it has been required a minimum production of 3 liters per day. Preliminary experimental campaigns, together with numerical analysis (by means of COMSOL Multyphysics software), are performed to evaluate the performance of the passive device. The experimental and modelling results are then illustrated, compared and commented. Furthermore, based on the previous outcomes, a detailed comparison between the two technology configurations (namely the active and the passive), which includes economic and energy analysis, is presented pointing out the relative pros and cons and the most suitable applications for both. Lastly, further improvements of the presented work are outlined.

Acknowledgements

I would like here to thank all the people that contributed and supported the realization of this thesis.

Firstly, I would like to thank my academic supervisor, Prof. Matteo Fasano that gave me the possibility to work on such an interesting and stimulating project. Secondly, my research supervisors: Prof. Eliodoro Chiavazzo for his availability and knowledge and Dr. Matteo Morciano which guided me along the whole realization of this work. Their help and encouragement has been fundamental to retrieve these satisfying results.

My greatest thankfulness goes to my family for having promoted my decisions and ambitions, also in this particular historical period. Their encouragements and efforts have been essential for me in order to achieve this result. I hope to never disappoint their expectations.

Gratitude goes also to my closer and further friends. Thanks to Riccardo and Luca for all the quality time spent together and for having been my second family in these last 2 years. Thanks to Andrea for supporting me since I was 8 and for being always present, despite the distance. Thanks to Piermarco, Emanuele, Luigi, Michela, Matteo and Alessandro for the long chats and for have lived next to me this master degree time. Lastly, I would like to thank Marta, despite the fact that our paths have separated, I've had the joy and the honor to spend most of this time with her and this fact will be never forgotten.

I hope to achieve future results with all of you at my side, Thank you.

Contents

1	Introduction	7
1.1	Water Scarcity	7
1.2	Water Supply	8
1.3	Desalination Systems	9
1.4	Active Systems	10
1.4.1	RO-Reverse Osmosis	10
1.4.2	MSF - Multi-Stage Flash	12
1.4.3	MED - Multi-Effect Distillation	14
1.4.4	MD - Membrane Distillation	16
1.5	Passive Systems	18
1.5.1	Solar Still	18
1.5.2	Advanced: Solar Steam Generator	20
1.6	Thesis Outline	20
2	Active technology: Simulink model of an MD plant	22
2.1	Sun subsystem	23
2.2	Collector subsystem	25
2.3	Control subsystem	29
2.4	Pipe losses subsystem	30
2.5	Storage subsystem	33
2.6	Auxiliaries subsystem	35
2.7	MD subsystem	36
2.8	Pre-heater subsystem	39
3	Passive technology: A low cost solution for desalination	42
3.1	Working principle	42
3.2	OHDC (Oman Humanitarian Desalination Challenge)	43
3.3	Experimental set-up	45
3.3.1	Composition	45
3.3.2	Assemble	47

3.3.3	Features and characteristics	50
3.3.4	Experimental layout	55
3.4	Theoretical model	57
4	Results	60
4.1	Active Plant	60
4.1.1	Constant inputs	61
4.1.2	ETC collectors	62
4.1.3	PSC collectors	66
4.1.4	Summary	69
4.2	Passive device	69
4.2.1	Numerical Analysis	69
4.2.2	Experimental results	77
4.2.3	Summary	80
4.3	Comparison of desalination performance	81
5	Conclusions and Future Works	83

List of Figures

1.1	Global water scarcity subdivided in physical or economical [2]	7
1.2	Earth's water distribution [3]	8
1.3	Renewable energies that can power desalination processes [7]	9
1.4	Desalination systems classification [8]	10
1.5	Comparison between osmosis and reverse osmosis [11]	11
1.6	Sketch of the RO desalination cycle [11]	11
1.7	Schematic of an MSF plant [16]	13
1.8	Scheme of MED plant [19]	14
1.9	Scheme of an MD plant coupled with a solar thermal system [21]	16
1.10	Different configurations of MD technology [23]	17
1.12	a) Direct bulk water contact b) Innovative 2D path [29]	20
2.1	Simulink model	23
2.2	Blocks contained in the sun subsystem	25
2.3	Evacuated Tube Collector device [33]	26
2.4	Parabolic Solar Collector [34]	26
2.5	Efficiencies of the different solar collector technologies, with x defined as in Equation 2.8	28
2.6	Solar collector subsystem	29
2.7	Control unit subsystem blocks	30
2.8	Pipe losses subsystem	32
2.9	Blocks in the Storage Subsystem	35
2.10	Auxiliaries subsystem blocks	36
2.11	MD unit subsystem blocks	39
2.12	Pre-heater subsystem blocks	41
3.1	(a) Schematic of the 3-stage distillation device (b) Detail of a single stage of distillation, showing the temperature, the activity (i.e salinity) and the vapour pressure gradients [43]	43
3.2	Logo of the challenge [45]	44

3.3	All the components necessary for the realization of a panel	46
3.4	MACOM VAC2060	47
3.6	Stratigraphy of one stage	49
3.7	Subdivision of the case areas once the transparent holders are glued.	50
3.8	Case with 2 devices and catheters installed	50
3.9	PV infinity ISOsun solar simulator	53
3.10	Salinity measurements by means of digital refractometer	54
3.11	Initial levels of water and after 24 hours of contact. It is possible to observe the impossibility of the particles passage across the membrane	54
4.1	Irradiance per collector surface in the first ten days of January a July	61
4.3	Capital cost of the different components	63
4.4	Scatter plot of the different configurations	64
4.5	Annual mean temperatures of the fluids evolving in the different sections of the plant considering the different configurations	64
4.7	Annual distillate water production in the 4 configurations	65
4.8	Capital cost of the different components	66
4.9	Scatter plot of the different configurations	67
4.10	Annual mean temperatures of the fluids evolving in the different sections of the plant considering the different configurations	67
4.12	Annual distillate water production in the 4 configurations	68
4.13	Geometry with detail	70
4.14	Black paint solar absorber emissivity [50]	73
4.15	Detail view of meshed model	73
4.16	Error plot	74
4.17	Diffuse water fluxes in the different stages	75
4.18	Volumetric temperature profile	76
4.19	Temperature drop across the device's height. (1) corresponds to an alu- minum substrate, (2) to an hydrophilic substrate and (3) to an hydrophobic substrate.	76
4.20	Section temperature distribution and thermal heat loss representation	77
4.21	Distillate mass and productivity over time of a single device	78
4.22	Evaporator's points for salinity measurement	79
4.23	Distillate mass and productivity over time of a single device	80
4.24	Distillate productivity comparison	81

List of Tables

1.1	Results of the most significant active processes	15
2.1	Data of the VTK 1140/2 ETC system [35]	27
2.2	Data of the Turbocaldo Innova PSC system [36]	28
2.3	Water, Glycol and Mixture properties [38]	29
2.4	Pipe line data	31
2.5	Seawater thermodynamic properties	34
2.6	Membrane data	37
3.1	Table showing the cost of the materials for one and five desalination panels	51
4.1	Chosen values for the different variables	60
4.2	Constant input parameters	62
4.3	ETC configurations and corresponding results	62
4.4	PSC configurations and corresponding results	66
4.5	Simulation water production results	75
4.6	Heat losses in the device	77
4.7	Salinities on the first evaporator and condenser over time	78
4.8	Salinities on the first evaporator and condenser over time	79
4.9	Comparison between the two technologies	81

1. Introduction

1.1 Water Scarcity

Even if almost 97% of the world's surface is covered by water, only the 3% of the total amount is fresh. This makes this primary resource rare, considering furthermore that two-thirds of this amount composes glaciers and so is unavailable for our use [1].

As a result one-third of the population faces "high baseline water stress" and one-quarter faces even "extremely high baseline water stress". These expressions were first used by UNESCO in the WWAP (World Water Assessment Programme) [2] in order to certificate the hydrological status of the world's different regions. This study consists in comparing the available water per year with the population which consumes it. When the annual available water is below $1700 m^3$, it is already considered water stress condition. If this value is lower than $1000 m^3$ high water scarcity occurs, instead if it is lower than $500 m^3$ extremely high water scarcity is present.

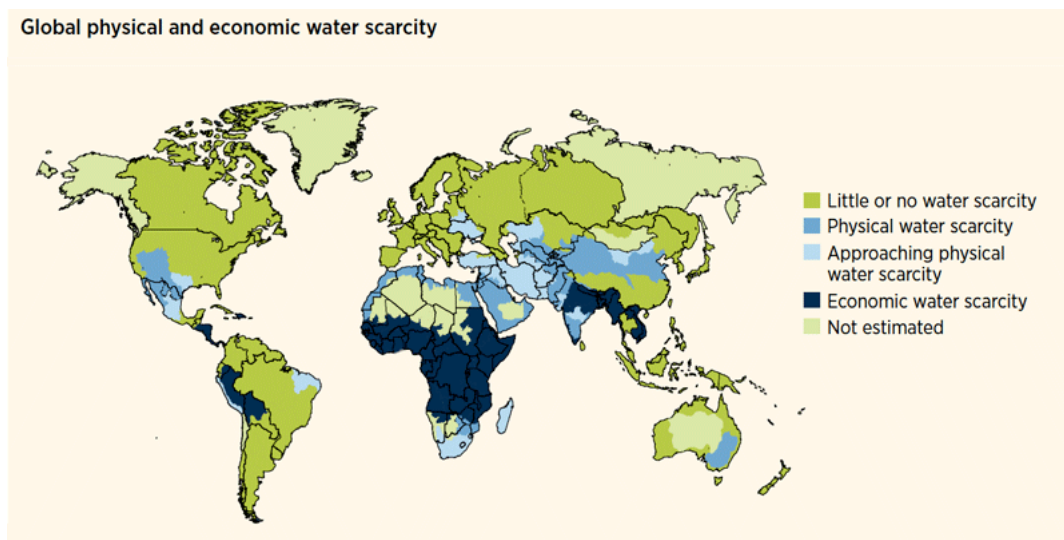


Figure 1.1: Global water scarcity subdivided in physical or economical [2]

Water scarcity can be subdivided in physical or economical. In the first case the lack of water is given by the environmental conditions of some specific regions, for example

arid zones located along the equator. In the second case instead, high poverty leads to a lack of infrastructures and workforce necessary to correctly provide water to the local population. Figure 1.1 shows where on earth economical or physical water scarcity are present.

Unfortunately the situation is worsened by the last century human behaviour. Due to pollution, intensive agriculture and population growth the presence of physical water scarcity in the globe is increasing year-by-year. The high levels of pollution dry up and contaminate the available fresh water basins, the wasteful use of water in agriculture empties aquifers and rivers and the population growth lead to an increase of water demand [1].

1.2 Water Supply

As already mentioned before only a little part of the global water can be used for human purposes. Furthermore, of the total 3% only the 0.3% is surface water easily accessible, the rest is located underground and several works must be computed in order to retrieve it (Figure 1.2).

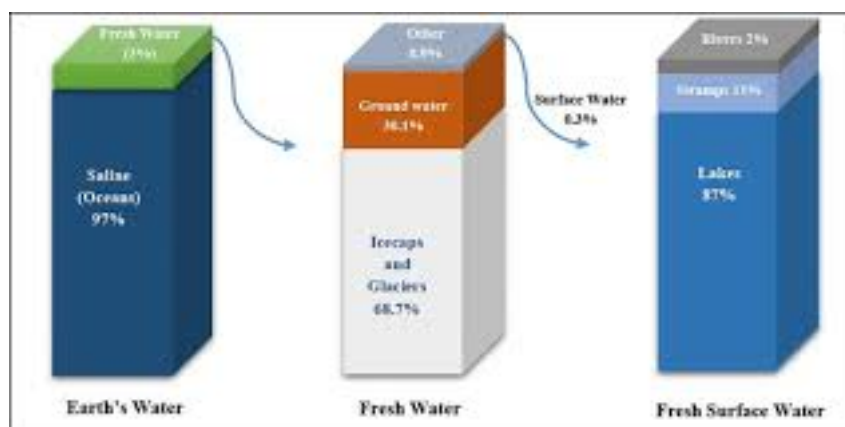


Figure 1.2: Earth's water distribution [3]

The totality of these water resources undergoes the so called *hydrologic cycle*, which consists of different steps leading to a sequence of evaporation and condensation phases. This cycle is important because it allows to regenerate fresh water in the different resources on earth. By means of this cycle, the different water basins can be distinguished in: renewable and non-renewable. In the first case this last it is able to regenerate in a short time span, for example the ground level water. Meanwhile in the second case, the time span is much longer than the previous one but is not infinite, for example polar ice and glaciers [4].

Due to this great lack of available fresh water many studies are in progress in order to widen the availability of water resources, in particular desalination which will be widely analysed in this text.

1.3 Desalination Systems

Desalination is a process which allows to remove minerals, in particular salt, from water. These systems contribute producing only 1% of the total potable water, due to their high energetic consumption (in high-pressure reverse osmosis plants to supply 300,000 people in a day, 31 MW are required [5]). Although, thanks to the advent of new technologies, desalination systems are becoming the most plausible alternative for fresh water production. Indeed some countries, with high physical water scarcity, as Kuwait and Qatar already produce the totality of their water by means of innovative desalination plants. Nevertheless nowadays the water, produced by desalination, costs about twice of the one retrieved from natural resources [6]. In order to reduce this cost and the environmental impact of these processes, scientists are studying an efficient way of implementing renewable energies as a primary source (Figure 1.3).

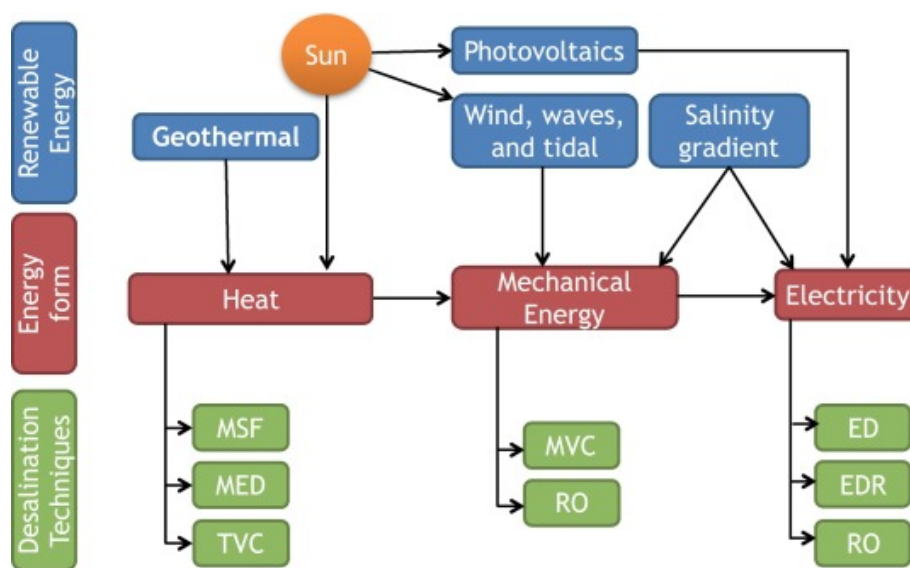


Figure 1.3: Renewable energies that can power desalination processes [7]

An important classification can be done between *thermal-based* and *membrane-based* systems (Figure 1.4).

Thermal-based technologies typically operate by evaporating water with thermal energy, and later condense it, leaving high salinity water (brine) as process waste. Membrane-based systems instead use physical obstacles and mechanical energy to separate the minerals from water. Thermal technologies are typically the most used especially in Middle-East

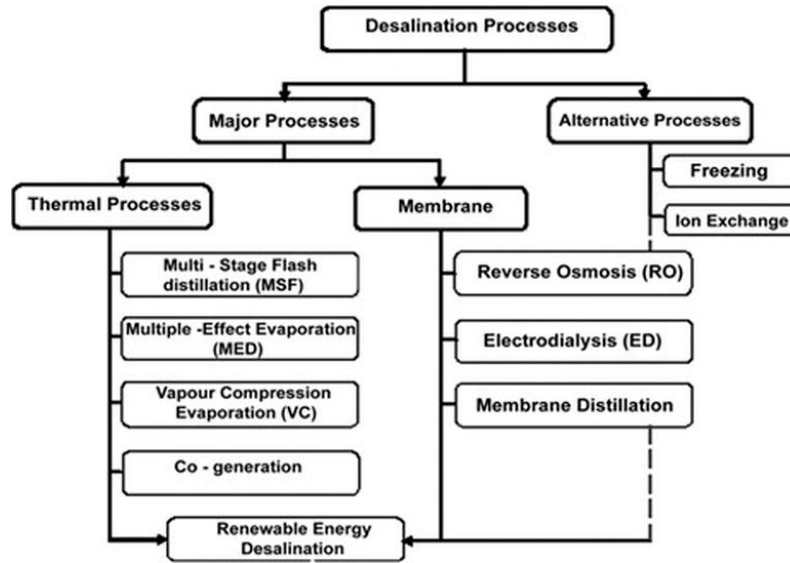


Figure 1.4: Desalination systems classification [8]

[9] where energy cost is lower, even if recently membrane systems have been reconsidered thanks to their: high energy efficiency, low space requirement and operational simplicity. Another big distinction can be done by subdividing desalination systems into *active* and *passive*. Whenever external energy sources are used to drive the desalination, we talk about active systems. Contrarily, if the working principle is mainly based on solar systems and insulating materials, with no use of external energy, we talk about passive systems. This last subdivision is the one that is gonna be used in the text, in particular in the next description of the most important and innovative desalination systems available.

1.4 Active Systems

1.4.1 RO-Reverse Osmosis

It is the most reliable and most commonly used desalination technique. It accounts for the 61% of the world's fresh water produced with desalination [10].

To better understand RO technique it is better to clarify how osmosis works. Osmosis is a natural phenomena where water molecules in a weaker saline solution tend to migrate towards a higher saline solution (Figure 1.5a). More in detail, if these two solutions are separated by a semi-permeable membrane (allows only some molecules to pass, for example only water and not salt) water molecules in the lower saline solution tend to migrate in order to lower the *chemical potential difference* previously established.

Reverse osmosis is the process of osmosis in reverse. External energy applied to the more saline solution is needed, in order to increase the chemical potential difference and obtain

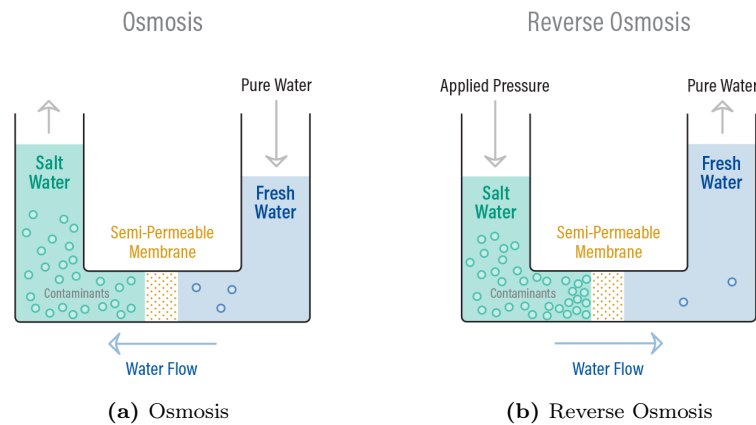


Figure 1.5: Comparison between osmosis and reverse osmosis [11]

a less saline solution (Figure 1.5b).

In a RO desalination plant the flow of water through the membrane is continuous and is provided by a pump. In particular three flows are present: feed, rejected and permeate flows (see Figure 1.6). The water contained in the first one is pressurized by the pump and sent against the membrane, holding a salinity which depends on the application. The second flow holds water with a salt concentration around 95% to 99% which was unable to pass, namely this water is defined *brine*. The last one instead contains the fresh water produced by the process, with a salinity much lower than the rejected one. The cross-filtration system allows to obtain 2 divergent flows when the inlet one encounters the membrane.

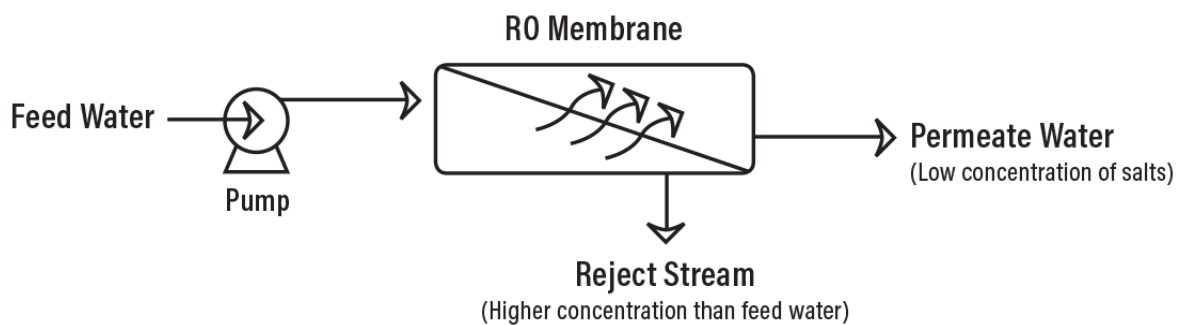


Figure 1.6: Sketch of the RO desalination cycle [11]

Some pre- and post-treatments must be done, in order to maintain the correct functioning of the device. For the purpose of avoiding pump clogging or membrane fouling, it is necessary to remove any possible inorganic suspended solid from water, by means of mechanical or chemical pre-treatments (for example coagulation, sedimentation and sand filtration) [12]. Thanks to these treatments pumps, can be used up to 100 bar with low risk of damage. Depending on the type of application some post-treatments may be needed, the most frequent are: pH adjustment, disinfection and remineralization.

The membranes which are typically used are: *hollow fiber*, *spiral wound*, *plate* and *tubular*, in particular the first two are preferred for their versatility and their cost related to the productivity. The pores in the membrane are large enough to let the water pass, but small enough to stop the salt molecules or blocks.

The RO technology is widely used because it has several advantages [13], some of them are:

- Easy design and operation of the plant;
- Modular nature, which allows modification of the plant's dimensions;
- Low maintenance if pre-treatments are present;
- Membranes can remove both organic and inorganic contaminants;
- Waste water is low;
- No thermal energy is required since the plant operates at ambient temperature, so less corrosion;
- Electricity is needed, so solar panels can be adopted;
- Specific power is the lowest among all the other technologies ($3-9.4 \text{ kWh/m}^3$);

Despite all these advantages also the RO technology has some drawbacks which limits its usage in specific situations. First of all, this process allows to obtain a low *recovery efficiency* (RE), defined as "ratio of the volume of desalinated water produced to feed water" [14], with values around 45% or less in other specific cases. This general inefficiency, compared to thermal desalination systems (MVC have RE of 97%), doesn't affect the total cost of the process when talking about large scale problems, although in scaled-up cycles usually the cost of RO tends to increase. An other important drawback of the technology is the great amount of energy required. Generally speaking this energy is given by fossil fuels (expensive and environmentally unfriendly), even if recently many attempts have been made in order to use renewable energy as main source.

Overall RO allows to obtain water at $0.5 \text{ \$/m}^3$ [15], with the price dropping year-by-year thanks to the advent of new technologies in the process.

1.4.2 MSF - Multi-Stage Flash

MSF is the most used thermal-based desalination technique and accounts for the 26% of the total distilled water produced [10].

This process bases its working principle on *flash evaporation*, which consists in a rapid evaporation of a saturated liquid stream when it undergoes a rapid reduction of pressure by passing through a throttling valve. A scheme of the plant is shown in Figure 1.7.

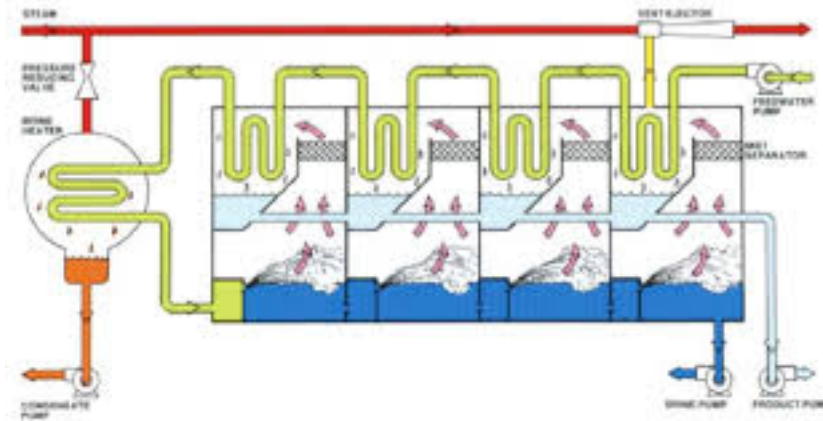


Figure 1.7: Schematic of an MSF plant [16]

In principle the seawater is withdrawn by a pump and sent in a multistage heat exchanger where heats up. Later the water is sent in a chamber where is further heated up by an external thermal source (fossil-fuel combustion or renewable energy) till it reaches 90-110 °C. At this point, the hot brine enters the stages of the device, at low pressure environment, and flash evaporate. The hot steam condenses releasing latent heat to the seawater previously introduced. Finally, both the freshwater and the brine are released by some pumps. A typical MSF system can have 4 to 40 stages, indeed the brine of the last stage will have a very high salinity, so will be treated as a waste.

Overall the system requires high amounts of electrical and thermal energy to produce the final fresh water. In order to reduce the environmental impact of the system, in modern plants are coupled renewable energy systems.

Some of the advantages of MSF are [17]:

- Simple working principle;
- Works well in large scale problems;
- Renewable energy sources can be easily integrated;
- Gives high quality fresh water (no more than 10 ppm);
- Needs no pre-treatment, except for filtration to remove solid materials;
- Cost effective where energy costs are low;

Generally this technology has a RE value around 25%, and have necessity of a high level of maintenance, with a consequent increase in the operational costs. In fact flash evaporation tends to produce deposits around the chamber, especially at the entrances. Another big disadvantage is the treatment of the wasted brine, which cannot be simply released in the environment since it could harm the local fauna and flora.

It is nowadays the most used technology in the gulf region, due to it's large scale feasibility with high efficiency and the low cost of fossil fuel in those areas. The water cost ranges between $0.52 \text{ \$/m}^3$ and $1.75 \text{ \$/m}^3$ [18].

1.4.3 MED - Multi-Effect Distillation

It is an older technology respect to the MSF, but it is still used to produce the 6% of the total distilled water [10].

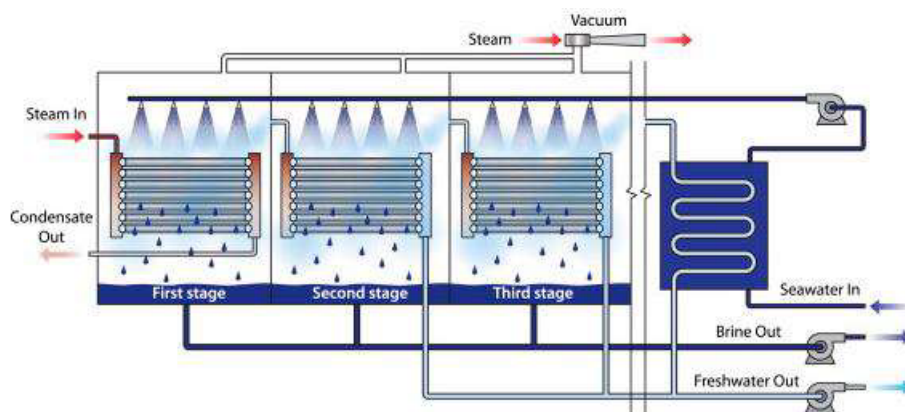


Figure 1.8: Scheme of MED plant [19]

Its working principle consists in transferring the latent heat of vapour multiple times so to condense fresh water and generate new vapour. By means of a pump the seawater is retrieved and sent to a preheater, in order to be initially heated up. Then the feed water is sent to the first stage of the plant, where is sprayed on a coil containing water at 70°C coming from another circuit. Most of the sprayed water instantly evaporates, then the vapour is collected and sent to the next stage through a new set of pipes. Having the vapour a lower temperature in the following stage, in order to assure again the seawater evaporation, the vessel pressure is decreased. The process is repeated several times, till at the last stage where the exceeding vapour is condensed in the preheating process. The seawater which has not evaporated is collected in every stage and expelled as process waste (brine). In Figure 1.8 it is shown a scheme of an MED plant.

Similarly to the MSF, the MED technology necessitates of thermal and electric energy to allow the correct desalination of water. These energies are usually taken by combustion

of fossil fuels, even if in the latest years renewable sources have been adopted to reduce the overall environmental impact.

The main advantages of the MED technology are [17]:

- Lower maximum temperatures respect to MSF, so less corrosion;
- Better production for low scale applications;
- Very compatible with solar auxiliaries;
- Power consumption is lower, thanks to the lower temperatures;
- No pre-treatment required except for filtration;

This technology reaches RE of 30%-50%, performing similarly to RO and better than MSF. Despite these advantages, this technology is not preferred due to some important drawbacks, here cited:

- Complexity of construction, so difficulty in scaling the plant;
- Low temperature of hot steam, which limits the choice of the thermal source;
- Output temperature must be at least as the environmental one to have condensation;

In particular the last disadvantage limits the amount of stages (dimensions of the plant) especially in hot areas, which are the ones more needy of fresh water. Principally for this reason the MED diffusion is limited.

Nowadays MED is being reconsidered thanks to the various hybrid configurations which allow to overcome some of the disadvantages. In particular: *Multi-Effect Distillation Absorption Desalination* (MEDAD), MED combined with thermal vapour compression (MED-TVC), *Boosted Multi-Effect Distillation* (B-MED) and *Flash-Boosted Multi-Effect Distillation* (FB-MED).

In average the water produced with this process costs from 0.7 $\$/m^3$ to 1.2 $\$/m^3$ [20].

Process	Thermal Energy [kWh/m ³]	Electric Energy [kWh/m ³]	Water costs [\$/m ³]
SWRO	//	3-4	0.5-1.2
MSF	7.5-12	2.5-4	0.7-1.2
MED	4-7	1.5-2	0.8-1.5

Table 1.1: Results of the most significant active processes

In conclusion Table 1.1 resumes all the values obtainable with the three active technologies illustrated, which cover 93% of the fresh water production.

1.4.4 MD - Membrane Distillation

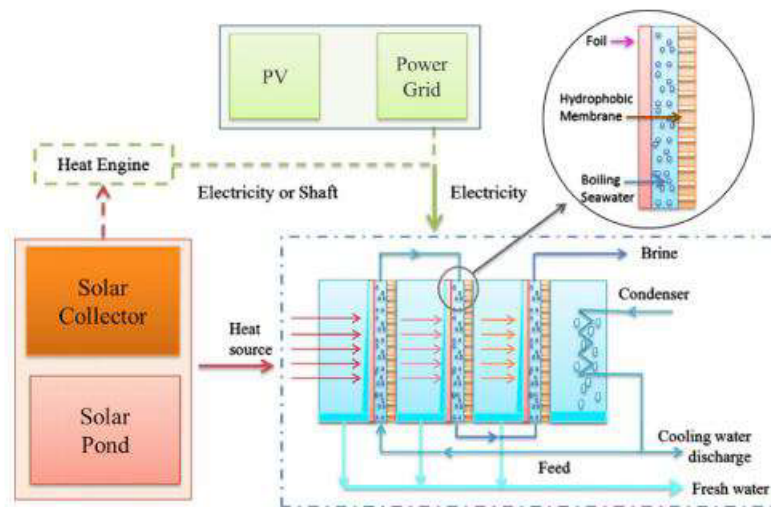


Figure 1.9: Scheme of an MD plant coupled with a solar thermal system [21]

MD is new desalination technology, but can be used also for treatment of wastewater and production of concentrate liquid. It covers only a small percentage of the desalination plants market, but recently it has gained interest thanks to the possibility of having a modular component design, which allows the use in remote areas. The scheme of a typical MD plant is shown in Figure 1.9.

MD technology bases its functioning on seawater evaporation across an hydrophobic membrane. At first, the feed water is sent, by means of a pump, into a channel which shares one side with a foil and the other side with an hydrophobic membrane. The particularity of this membrane is that allows the passage of vapour, but inhibits the water's one. Once evaporation is triggered, by the foil in contact with a heating source, the vapour produced passes through the membrane leaded by a pressure gradient, in turn generated by the preexisting thermal one. At last, the vapour collected in the adjacent chamber condenses in contact with a second foil, and is then retrieved by a second pump. The latent heat of condensation is used for a second evaporation, repeating the cycle for the remaining stages. The number of stages of the device depends only on the amount of heat provided by the heating source.

Generally speaking the MD technology can be subdivided in four types [22] (Figure 1.10):

- **DCMD** (Direct Contact Membrane Distillation). Both the vaporizing and the condensing fluids are in contact with the membrane. The generated vapour passes driven by a pressure difference between the two sides. Commonly used configuration, even if a conspicuous amount of heat is lost in the process, due to conduction.

- **AGMD** (Air Gap Membrane Distillation). The vaporizing fluid is still in contact with the membrane, but an air gap is interposed in between this last and the condensing liquid. Vapour flux is always present, but the transfer velocity is reduced. The air acts as a resistance and limits the dispersion of heat, given by conduction.
- **SGMD** (Sweeping Gas Membrane Distillation). In this case a cold gas is sent tangentially to the permeate side of the membrane, in order to collect the vapour produced and bring it to an external condenser. In this way condensation is performed externally, so heat lost is limited and vapour transfer velocity is enhanced. The main drawback is the diffusion of vapour in the gas, which leads to the necessity of a bigger condenser.
- **VMD** (Vacuum Membrane Distillation). Has the same working principle as SGMD, but uses vacuum instead of a gas. Heat losses are minimal, even if the process requires an additional pump to work. Indeed capital and operational costs are higher.

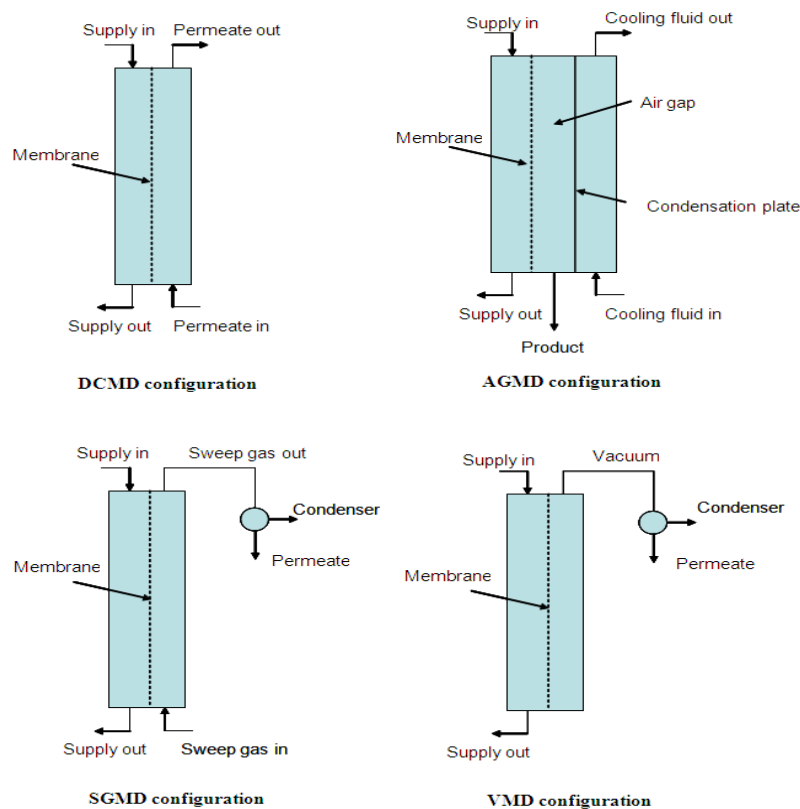


Figure 1.10: Different configurations of MD technology [23]

Also MD is a thermal based technology. The main reason why it is considered so interesting, is the great possibility of satisfying the energetic needs of the process by means

of renewable sources. This is thanks to the low temperatures reached ($\sim 80^\circ\text{C}$) for the evaporation of the fluid.

The advantages are here resumed [22]:

- MD membranes are cheap and robust. Low necessity of pre-treatments;
- No corrosion problems;
- High quality of distilled water, considering also non-volatile elements;
- Low electrical consumption during operation;
- Low complexity of the apparatus;
- Low maintenance;
- Temperatures and pressure levels are lower than in other desalination technologies;
- Process can be easily coupled with renewable energy sources;

The main drawback which still limits the diffusion of this technology, is the high cost of fresh water produced. In fact, despite the low temperatures, the heat required is high and the permeate flux is low, which leads to a high cost of water production. The typical value of thermal energy required is $100 \text{ kWh}/\text{m}^3$ [24], which turns out to be high if compared to the values reported in Table 1.1.

1.5 Passive Systems

There are many passive systems in the state of art or which are in development. The most conventional one is the solar still, which can be implemented and advanced in many solutions, the one reported in this text is the solar steam. For sake of simplicity only these latter will be analysed, meanwhile the designed device's working principle, namely Membrane Distillation, will be largely discussed in Section 3.

1.5.1 Solar Still

Is the most ancient form of desalination, and consists of evaporating seawater by means of solar energy, replicating the way nature makes rain.

A typical configuration consists in a container, having at the bottom an insulated layer covered with seawater, and at the top a tilted transparent surface (typically glass). As the solar radiation enters heating up the seawater, the vapour rises up and condenses in contact with the tilted surface. Finally the droplets formed slide along the surface and

are collected apart. Thanks to the fact that the container is closed this type of technology adopts the greenhouse effect to better evaporate the seawater contained inside. In Figure 1.11a is possible to observe the standard device configuration.

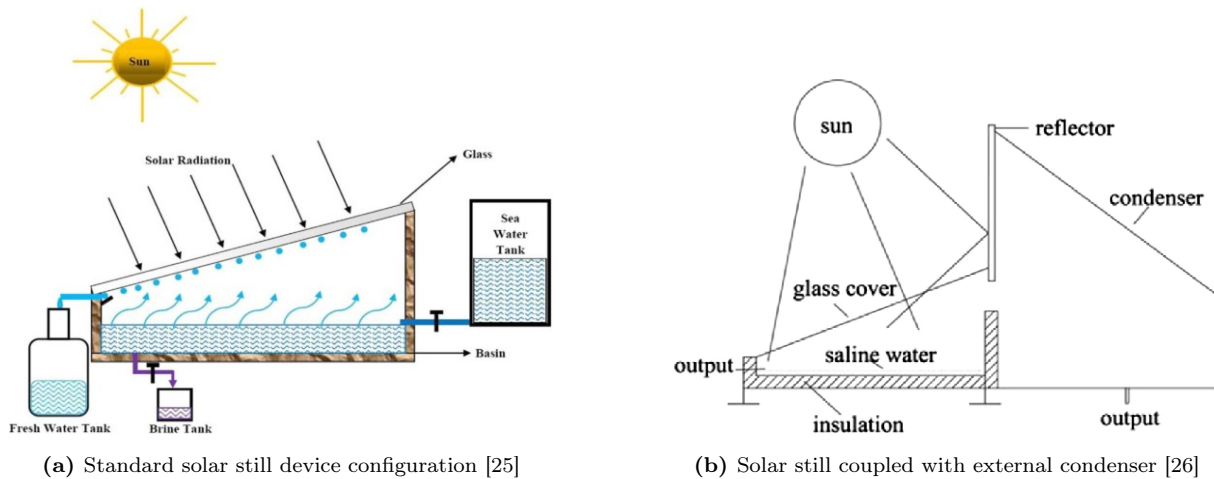


Figure 1.11: Different solar still configurations

A part from the basic ones, the solar still technology can assume different configurations [21]:

- **Single stage device**, as the one previously described;
- **Solar still coupled with collectors**, in this case some collectors are used to pre-heat the seawater in order to increase the efficiency of the device;
- **Solar still coupled with condenser**, a further condenser is used to increase the condensate production (Figure 1.11b);
- **Multi-stage solar still**, many stages are present in order to recover the latent heat of condensation;

Generally speaking this type of technology is not adopted for industrial water production purposes, since its productivity is proportional to the device's area. Unless building big plants (which is not economically convenient), this technology water productions are limited. Nevertheless, thanks to the high water quality and portability, this last is typically employed in remote and arid regions [27]. Furthermore, the facility of maintenance and low operational costs enhance the usage in these regions.

As we are talking of passive devices the "cost of water" as parameter for the performances loses of sense, since the production depends on external variable factors (solar irradiation, wind, ecc.). In order to evaluate the device's efficiency, the productivity of water per day is considered. In this specific case, with a mean solar irradiation of 700 W/m^2 , the device exploits a mass flow rate of $0.936 \text{ L/(m}^2\text{h)}$ [28].

1.5.2 Advanced: Solar Steam Generator

Also this technology uses the solar energy to produce distilled water. It is not suitable for large productions, but is capable of reaching high productivity rates. During the process the system dissipates a lot of energy to the bulk water with which the solar absorber is in contact. Due to this fact, the scalability of the system is limited, with a consequent impossibility of industrialization.

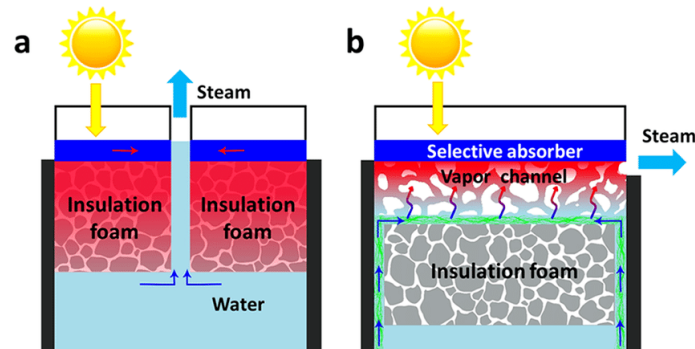


Figure 1.12: a) Direct bulk water contact b) Innovative 2D path [29]

An innovative configuration limits the energy dissipation, opening a new road for further implementations of the system. The idea consists in a floating thermal insulator standing alone in the bulk water, wrapped in a super-hydrophobic foil. Saltwater is absorbed in the layer thanks to capillarity, until it reaches the top where evaporates thanks to the solar energy collected by the absorber. The solar energy used is maximized, as all of it is employed in water evaporation. The overall construction of the device is then shown in Figure 1.12.

The productivity of the technology reaches a maximum of $1.45 \text{ L}/(\text{m}^2\text{h})$ under a mean solar irradiation of $1000 \text{ W}/\text{m}^2$. This value is the one of the highest reachable nowadays with passive technologies.

1.6 Thesis Outline

After this short introduction of the different state-of-art active and passive desalination technologies, it is important to expose how this thesis is structured. The second chapter illustrates the Simulink design of a MD plant coupled with solar collectors and energy storage. In the following chapter, are illustrated the prototyping and the design of a passive desalination device based on MD technology. The fourth chapter collects the results of the two models, retrieved by experimental campaign and numerical simulations, and the comparison between the two technologies. The last chapter instead holds the conclu-

sions, where the feasibility of the MD technology in passive devices and the application cases of both the desalination apparatus are considered.

2. Active technology: Simulink model of an MD plant

This model aims to compute the total amount of fresh water produced in a year by a solar desalination system, working by means of membrane distillation. This last has a dynamic behaviour due to: the hourly variation of irradiance (that influences the amount of disposable heat) and the inertia of the storage system. For this reasons it has been employed Simulink as simulation software, since it is capable of dealing with high dynamic systems. Simulink works with *blocks*, owing *input ports* and *output ports*, and *signals* transferred from a block to another. Inside these blocks it is possible to execute many operations, mathematical and logical. A group of blocks can be collected in a *Subsystem*, according to the user's desire, as in this case where the different subsystems represent the components of the plant.

The composition of the proposed system is the following:

- **Sun Subsystem:** the irradiation per unit of area is evaluated, starting from the solar data provided by the European Union;
- **Collector Subsystem:** the solar irradiation is converted into heat and transferred to water flowing inside the collectors;
- **Control logic subsystem:** a logic control is computed on the collector's and storage water, guaranteeing the best performances of these devices and preventing dangerous situations (i.e water temperature > 100 °C);
- **Pipe subsystem:** simulates the flow of water in a pipe line, calculating the consequent heat losses;
- **Auxiliaries subsystem:** a logic control assures a minimum temperature to the MD module inlet water, so to avoid physical incoherences;
- **MD module:** mimics a MD desalination unit, converting hot saltwater into cooler freshwater;

- **Pre-heater:** simulates the behaviour of a heat exchanger, useful to recover part of the latent heat unused during the desalination process;

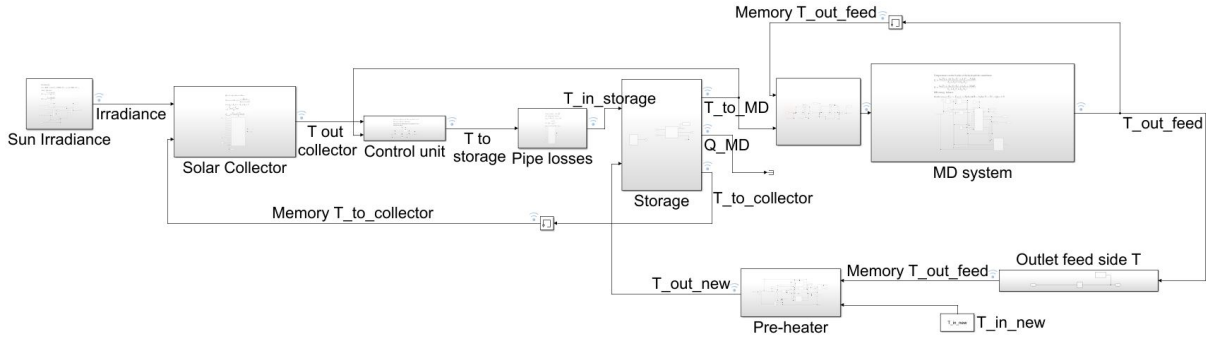


Figure 2.1: Simulink model

The presented model simulates the functioning of the system, considering every time step as an hour of usage of the apparatus. This choice allows to reduce the computational cost, without reducing the correctness of the obtained results. Furthermore, the simulation incorporates five years of usage, in order to avoid that the transient phase compromises the real obtained results (only the last year is taken in consideration in the results). To solve the problem, Simulink automatically decides the type of solver depending on the complexity and in this case the solver *ode3* (Bogacki-Shampine method) has been used. In the following sections every subsystem of the model will be analysed in detail.

2.1 Sun subsystem

The main purpose of this subsystem is to compute the hourly solar irradiation, at a certain position on Earth, incident on the collectors surface. The irradiation data are collected from the Photovoltaic Geographical Information System (PVGIS) of the European Commission [30], which provide a Typical Meteorological Year (TMY) of the selected location. This last is a non-existing year containing meteorological data, obtained by an analysis of previous several years of the selected place. The interesting parameters for this thesis are: the dry bulb temperature, the Global Horizontal Irradiance (**GHI**), the Diffuse Horizontal Irradiance (**DHI**) and the Beam Normal Irradiance (**BNI**).

In order to obtain the wanted results, two steps must be performed: the irradiance on the collectors must be computed (considering this last inclination and view factors) and then must be computed the radiation considering the irradiance, constant during the hour.

The equation used to evaluate the irradiance (G) on a tilted surface is [31]:

$$G = BNI \cdot \cos \theta + DHI \cdot F_{c-s} + \rho \cdot GHIF_{c-g} \quad (2.1)$$

where:

- θ is the angle formed between the BNI and the surface, and it allows to evaluate the portion of irradiation which reaches the surface;

- F_{c-s} is the view factor between the collectors and the sky:

$$F_{c-s} = \frac{1 + \cos \beta}{2} \quad (2.2)$$

- F_{c-g} is the view factor between the collectors and the ground:

$$F_{c-g} = \frac{1 - \cos \beta}{2} \quad (2.3)$$

- ρ is the albedo, indicating the fraction of irradiance which is mirrored by the ground and reaches the collectors;

- β is the angle formed between the collector surface and the horizontal plane;

In practice the value of θ is not directly evaluated, but the cosine is considered by equation [32]:

$$\begin{aligned} \cos \theta = & \sin \delta \sin \phi \cos \beta - \sin \delta \cos \phi \cos \gamma \sin \phi + \\ & + \cos \delta \cos \phi \cos \beta \cos \omega + \cos \delta \sin \phi \sin \beta \cos \gamma \cos \omega + \cos \delta \sin \beta \sin \omega \end{aligned}$$

where:

- δ is the solar declination, the position of the Sun at noon respect to equator plane (varies between -23.45° and 23.45°);
- ϕ is the latitude (positive towards North);
- γ is the azimuth angle, between the South direction and the projection of the normal to the surface on the horizontal plane (positive clockwise);
- ω is the hour angle, evaluated considering that each hour the Earth rotates of 15° (negative in the morning);

ϕ and γ depend on the geometry of the system, meanwhile ω and δ on the position of the Sun, in particular this last can be evaluated by means of the Cooper formula [32]:

$$\delta = 23.45 \sin \left(360 \frac{284 + n}{365} \right) \quad (2.4)$$

with n the day of the year.

The subsystem solves these calculations for every hour, providing as output the irradiance on the collector. The blocks of the subsystem are shown in Figure 2.2.

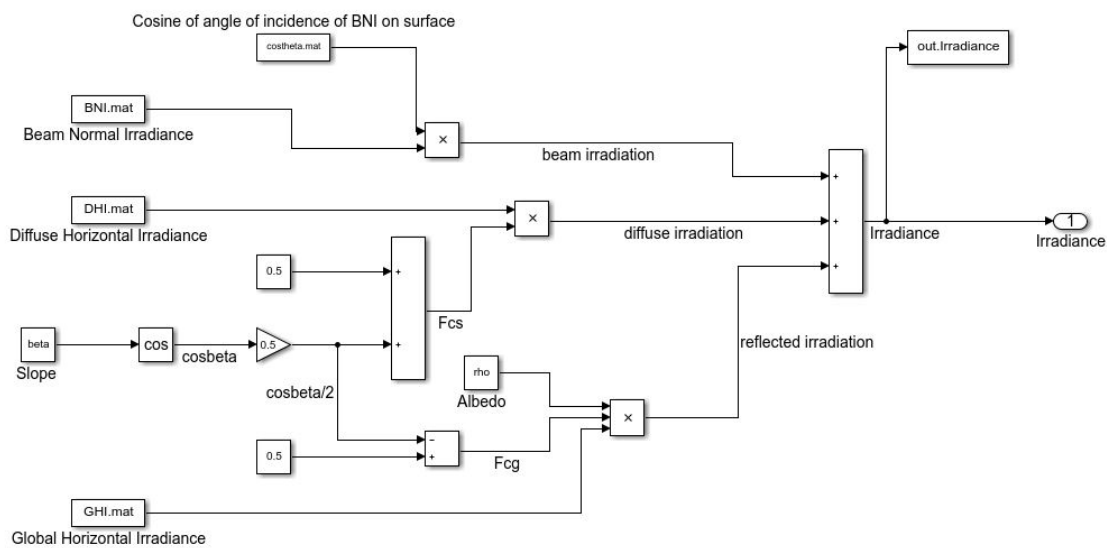


Figure 2.2: Blocks contained in the sun subsystem

2.2 Collector subsystem

The purpose of this subsystem is to convert the incoming irradiance into thermal heat delivered to a fluid flow.

Generally speaking, a solar collector is a particular type of heat exchanger, which uses solar irradiation to heat up a stream of fluid (commonly air or water), consequently delivered to a final user. Typically this fluid is used to feed Domestic Hot Water (**DHW**), low-temperature space heating or air conditioning plants. The exit temperature of the fluid from the collector depends on the climatic situation of the designated location and the device's efficiency. Usually the maximum temperatures reached range between 70 and 160 °C. Collectors are installed in places where they can be irradiated for the longer time possible along the day, therefore typically on walls, rooftops and on the floor in case of big installations.

In this application two different types of solar collector have been used: Evacuated tube collectors (**ETC**) and Parabolic solar collector (**PSC**). The first type consists in an absorber plate, which collects the solar irradiation, contained in a cylindrical glass tube having vacuum inside, together with a copper tube where the fluid flows. This particular configuration allows to reduce the convective dispersion of the plate, and enhance the heat transmission to the fluid (temperatures reached 140-160 °C), see Figure 2.3. The main disadvantages of this technology are: bad optical efficiency (cylindrical shape of the vacuum tubes) and part of the solar irradiation is not collected because of the gaps between the different tubes.

The PSC instead consists of a parabolic reflecting surface ($\sim 10 \text{ m}^2$), which conveys all



Figure 2.3: Evacuated Tube Collector device [33]

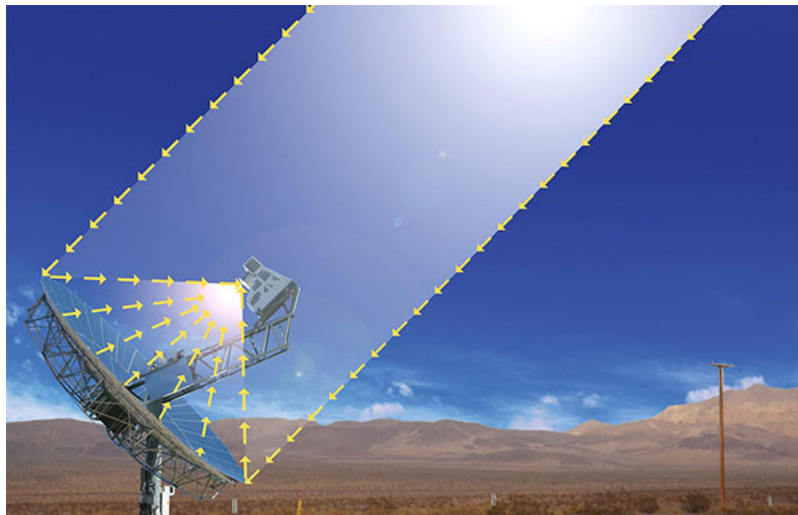


Figure 2.4: Parabolic Solar Collector [34]

the solar irradiation on a receiver where the evolving fluid flows and heats up (Figure 2.4). This technology has higher efficiency at the same area, respect to the other technologies, thanks to: the implemented sun tracking and the possibility of conveying the solar power in a limited area. The big disadvantage is the high cost of the device, which could not justify the higher capacities of the technology.

As already mentioned one of the main parameters to take under consideration when considering solar collector is the efficiency η , defined as [32]:

$$\eta = \frac{\int \dot{Q}_{u, coll} dt}{A_{coll} \int G dt} \quad (2.5)$$

where $\dot{Q}_{u, coll}$ [W] is the power generated by the device and A_{coll} [m²] is the collector's

area. Furthermore the power generated can be calculated through equation [32]:

$$\dot{Q}_{u,coll} = A_{coll}[G - U_L(T_{m,plate} - T_{amb})] \quad (2.6)$$

where U_L [$W/(m^2K)$] is the loss coefficient, $T_{m,plate}$ [K or °C] is the mean temperature of the absorbing plate and T_{amb} [K or °C] is the ambient temperature.

Generally speaking most of the manufacturers provide an experimental formula to evaluate the efficiency:

$$\eta = \eta_0 - c_1x - c_2G_kx^2 \quad (2.7)$$

where η_0 represents the optical losses due to the glass cover and c_1 , c_2 and G_k ($800 W/m^2$) are constants. x is defined as:

$$x = \frac{T_{m,coll} - T_{amb}}{G_k} \quad (2.8)$$

$$T_{m,coll} = \frac{T_{in,coll} + T_{out,coll}}{2} \quad (2.9)$$

Resuming, the equations solved in the Collector subsystem are:

$$\dot{Q}_{u,coll} = \eta A_{coll} I_T \quad (2.10)$$

$$T_{out,coll} = T_{in,coll} + \frac{\dot{Q}_{u,coll}}{\dot{m}_{coll}c} \quad (2.11)$$

where c [$J/(kgK)$] is the specific heat of the heat transfer fluid, \dot{m}_{coll} the collector mass flow rate and $I_T = G \times 3600$ [J/h].

The chosen devices are: model VTK 1140/2 (manufactured by Vaillant) and Turbocaldo (manufactured by Innova Energy Solutions). The main characteristics are collected in Tables 2.1 and 2.2.

	VTK 1140/2
η_0 [%]	64.2
c_1 [$W/(m^2K)$]	0.885
c_2 [$W/(m^2K)$]	0.001
Absorbing Surface [m^2]	2
Volumetric flow rate [l/h]	48

Table 2.1: Data of the VTK 1140/2 ETC system [35]

	Turbocaldo Innova
η_0 [%]	79.6
c_1 [$W/(m^2K)$]	0.66
c_2 [$W/(m^2K)$]	0.008
Absorbing Surface [m^2]	9.58
Mass flow rate [kg/h]	576.29

Table 2.2: Data of the Turbocaldo Innova PSC system [36]

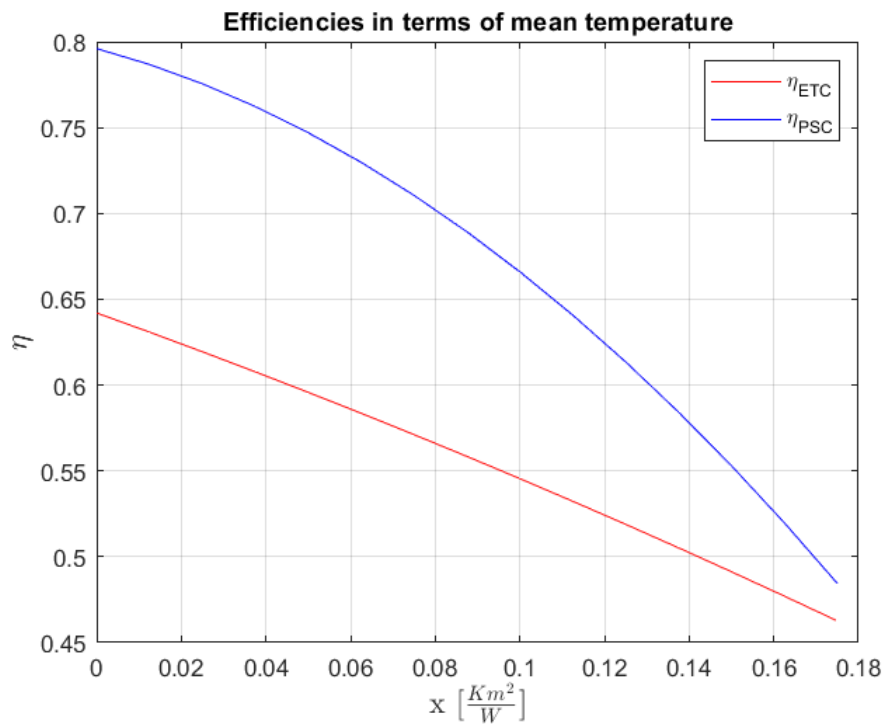


Figure 2.5: Efficiencies of the different solar collector technologies, with x defined as in Equation 2.8

In Figure 2.5 are represented the efficiencies for the different technologies, as the parameter x changes.

The fluid flowing in the collectors is a mixture of propylene glycol and water, respectively 20% and 80%. The properties of the two compounds and of the mixture are listed in Table 2.3.

As shown in Figure 2.6 the entire subsystem is constituted by a single *Matlab block*, which recalls a written Matlab function necessitating input information, and giving as an output the final temperature of the high temperature fluid.

	Water [37]	Glycol [37]	Mixture
Specific heat [J/kgK]	4186	2480	3843
Density [kg/m^3]	1000	1036	1007
Dynamic viscosity [$Pa \cdot s$]	10.7×10^{-4}	5.76×10^{-4}	9.72×10^{-4}
Thermal conductivity [$W/(mK)$]	0.599	0.201	0.519

Table 2.3: Water, Glycol and Mixture properties [38]

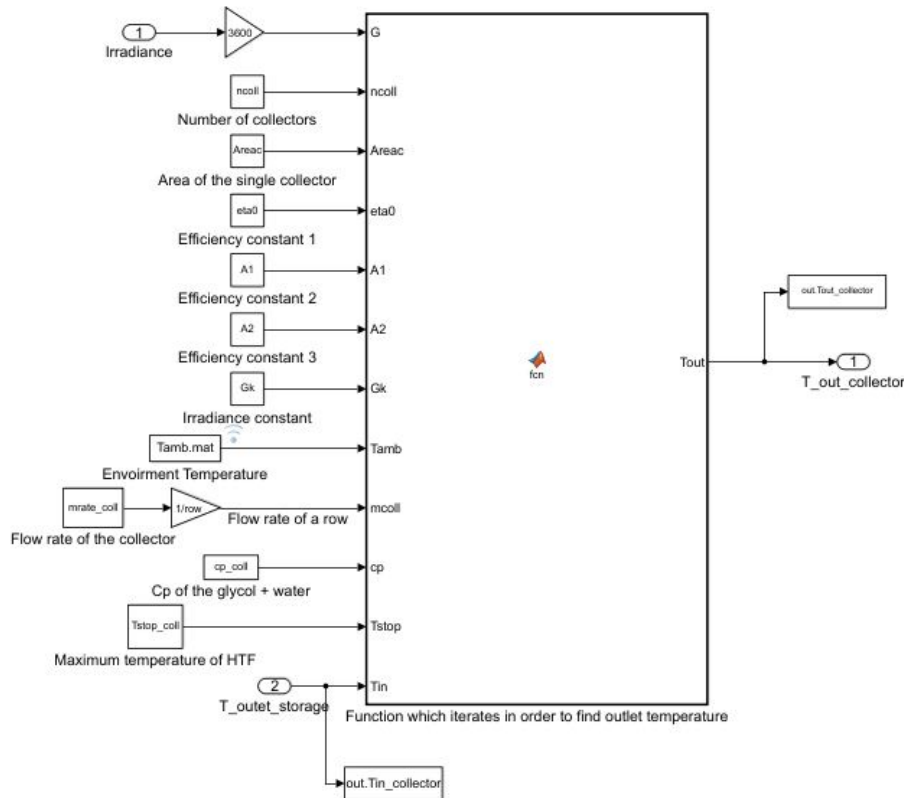


Figure 2.6: Solar collector subsystem

2.3 Control subsystem

Most of the control units which regulate the correct functioning of the plant are collected in this subsection. In real plants, this apparatus is constituted of thermostats and programmable units, which measure and compare the different signals, activating and deactivating the users depending on the required necessities. In this specific case, the subsystem manages the flows inside the collectors and the temperature in the storage unit.

The controls executed are here listed:

1. Temperature of the high temperature fluid, in order to limit the presence of high

temperatures, which could lead to damaging;

2. Measure the storage temperature, so to prevent the eventual cooling down of the storage fluid if the HTF has a lower temperature;

The subsystem adopts a logic language to deal with the previously cited controls. At first, the collectors outlet temperature is compared with the imposed threshold (i.e 100 °C). Then, the storage temperature is compared with the collectors outlet temperature, if $T_{out, coll} - T_{storage} > 2$ °C then the flow is allowed to go in the storage unit. Furthermore, the storage temperature is held lower than the maximum temperature suggested by the manufacturer. Lastly, the temperature of the new seawater coming from the pre-heater is compared with the storage temperature, if $T_{out, pre-heater} - T_{storage} > 2$ °C the flow is allowed to enter.

In Figure 2.7 are shown the different blocks.

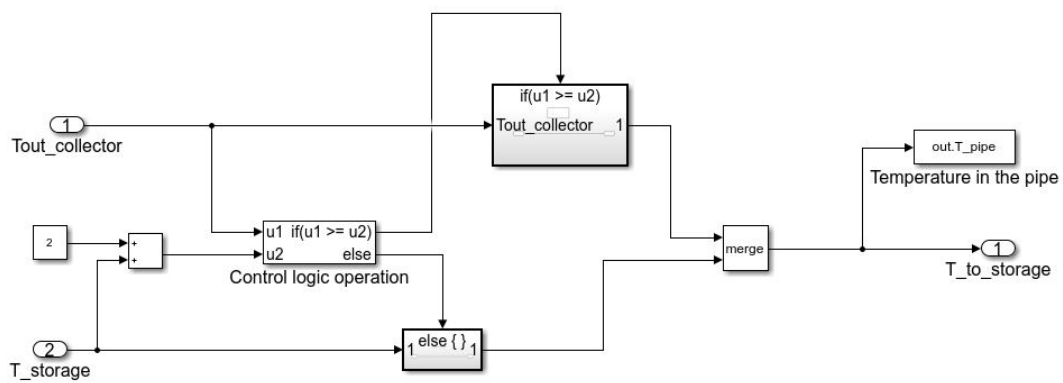


Figure 2.7: Control unit subsystem blocks

2.4 Pipe losses subsystem

This subsystem evaluates the heat dispersion during the passage of the hot fluid from the collectors to the storage tank.

The distance of these pipe lines depend on the specific type of application, in this case it has been hypothesized the installation of the collectors on a four-floors building, and the storage system placed at ground floor. Furthermore, in order to reduce the heat losses, a coating of glass wool for the pipes has been considered. All the data for the pipe line are collected in Table 2.4.

In order to evaluate the total lost heat, conduction and convection heat transfer must be considered. From the characteristics of the materials employed, it is already know the thermal conductivity of the insulator. To fully describe convection, it is necessary to

Pipe line data	
Length of the pipe line [m]	12
Pipe diameter [m]	15×10^{-3}
Thermal conductivity of glass wool [W/(mK)]	0.039

Table 2.4: Pipe line data

retrieve the convective heat transfer coefficient by means of the Nusselt number, which represents the ratio between convection and conduction in a physical medium. In particular:

$$Nu = \frac{hd}{k} \quad (2.12)$$

where: h [W/(m²K)] is the convective heat transfer coefficient, d [m] is the tube diameter and k [W/(mK)] is the thermal conductivity. From literature it is possible to retrieve the Nusselt number from empirical equations, depending on the present type of flow. In particular:

- **Laminar Flow:**

$$Nu = 3.66 \quad (2.13)$$

- **Turbulent Flow:**

$$Nu = 0.023Re^{0.8}Pr^n \quad (2.14)$$

In this application Equation 2.14 will be considered, where:

- Re is the Reynolds number, representing the ratio between inertial and viscous forces:

$$Re = \frac{\rho vd}{\mu} \quad (2.15)$$

- Pr is the Prandtl number, representing the ratio between momentum and thermal diffusivity:

$$Pr = \frac{c\mu}{k} \quad (2.16)$$

- n is a constant equal to 0.3 if the fluid is cooling, or 0.4 if the fluid is heating;
- ρ [kg/m³] is the density;
- v [m/s] is the mean velocity of the fluid in the pipe;
- μ [Pa · s] is the dynamic viscosity of the fluid;

Once know the convective heat transfer coefficient, in order to consider the lost heat, the pipe has been subdivided in infinitesimal portions, where it is reasonable to consider temperature $T_{in,i}$ constant. Furthermore, the external surface of the insulating material has been considered at ambient temperature, adopting a conservative approach. At the end the lost heat, for an infinitesimal portion, can be written as:

$$\dot{Q}_{lost,i} = U A_{in} (T_{in,i} - T_{amb}) \quad (2.17)$$

$$\dot{Q}_{lost,i} = \dot{m}_{coll} c_{mix} (T_{in,i} - T_{out,i}) \quad (2.18)$$

$$U = \left[\frac{1}{h} + r_i \frac{\log\left(\frac{r_i}{r_e}\right)}{k_{ins}} \right]^{-1} \quad (2.19)$$

where: U [$W/(m^2K)$] is the global heat transfer coefficient, A_{in} [m^2] is the internal area of the pipe, r_i and r_e [m] are respectively the internal and external radii of the pipe, k_{ins} [$W/(mK)$] is the thermal conductivity of the thermal insulator, c_{mix} [$J/(Kkg)$] the specific heat of the mixture and \dot{m}_{coll} [kg/s] the mass flow rate.

Combining Equations 2.17 and 2.18, it is possible to express the outlet temperature of the infinitesimal portion as:

$$T_{out,i} = T_{in,i} - \frac{1}{\dot{m}_{coll} c_{mix}} [U A_{in} (T_{in,i} - T_{amb})] \quad (2.20)$$

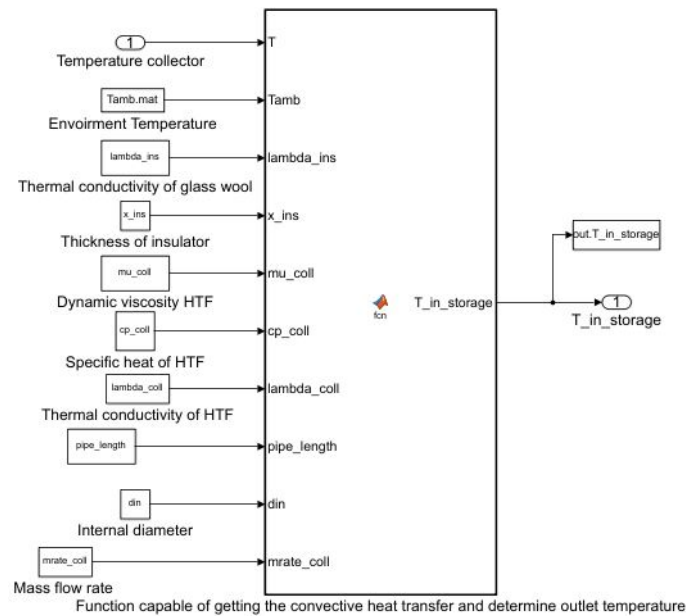


Figure 2.8: Pipe losses subsystem

Executing this calculation multiple times, it is possible to obtain the final outlet temperature of the fluid incoming in the storage system. In Figure 2.8, it is possible to notice that also in this case, it is present a Matlab block to solve the above mentioned iterations.

2.5 Storage subsystem

Since the solar energy is intermittent during the day, it is important to design a system capable of storing it, so to assure a more constant production of fresh water. Usually these systems consist of a tank full of a fluid, which must be characterized by a series of features. Generally speaking, the equation that governs the heat storage is:

$$Q = mc(T - T_0) \quad (2.21)$$

where Q [J] is the stored heat, m [kg] is the mass of fluid inside the storage system, c [$J/(kgK)$] the specific heat of the fluid and $(T - T_0)$ [K] is the difference between the actual and the initial temperature of the fluid.

As already mentioned, the fluid must have some characteristics, which are meant to maximise the energy storage and minimize the amount of storage volume required. Considering that the temperature of the fluid must be held in a certain range, these features are here listed:

1. The apparatus must not experience changes of state during usage (i.e liquid to vapour), unless explicitly required for the functioning of the plant. As a consequence, the variation of density ρ of the medium is limited, indeed is not an issue for the stability of the storage system;
2. The selected range of working temperature must assure no state change;
3. The specific heat of the fluid must be as high as possible (Equation 2.21), in order to reduce the dimensions of the apparatus;
4. Good thermal conductivity, to enhance the heat transfer;
5. Low toxicity and corrosivity, to assure operational safety and a long life of the storing tank;
6. Low cost, to make the investment sustainable;

Analysing the previously features, water results being the best choice, to overcome all these necessities. Indeed, this last: has one of the highest specific heat in nature ($c_{water} = 4186 J/(kgK)$), is easy to retrieve, cheap and non-toxic.

Considering this application, it has been chosen to adopt directly seawater as medium for the storage system. In fact, this last has slightly lower specific heat than fresh water (see Table 2.5), but adopting this choice the total cost of the plant is lower, since it is possible to eliminate an additional heat exchanger.

Seawater Data	
Salinity [g/l]	35
Density [kg/m^3]	1024
Specific heat [$J/(kgK)$]	3998

Table 2.5: Seawater thermodynamic properties

The storage system has been considered mixed, this presuppose that the fluid's temperature depends exclusively on time, and not on the position ($T = T(t)$). To determine the reached temperature of the fluid over time, a first principle analysis has been carried out, considering the different contributions.

A positive contribution is given by the heat provided by the mixture coming from the collector subsystem. Since the two fluids cannot be mixed, the heat transfer is performed by means of a plate heat exchanger [39], which operate in counter-current flow, and thanks to an $\epsilon - NTU$ analysis (passages visible in Section 2.8) it has been possible to derive the fraction of heat capable of being transferred.

In particular, the heat provided by the collectors can be expressed as:

$$Q_{coll} = \epsilon \dot{m}_{coll} c_{mix} (T_{mix} - T_{storage}) \quad (2.22)$$

Applying a thermal balance to the heat exchanger (assuming the same mass flow rates), it is possible to determine the mixture temperature going back to the collector subsystem:

$$T_{tocoll} = T_{mix} - \frac{Q_{coll}}{\dot{m}_{coll} c_{mix}} \quad (2.23)$$

Furthermore, a negative contribution is given by the heat lost to the environment during usage. It has been considered an insulating glass wool around the storage tank, so considering convection and conduction the total heat can be expressed as:

$$Q_{loss} = U A_{tank} (T_{storage} - T_{amb}) \quad (2.24)$$

where A_{tank} [m^2] is the external area of the tank, U [$W/(m^2K)$] global heat transfer defined as in Equation 2.19 (cylindrical tank). For simplicity the top and bottom surface heat transfers have been omitted, since their contribution are much lower than the considered one.

Lastly, another negative contribution is given by the heat delivered to the MD unit. This last can be computed considering the heat transferred during the desalination process and the pre-heating. In particular:

$$Q_{toMD} = \dot{m}_{toMD} c_{sw} (T_{storage} - T_{from,preheater}) \quad (2.25)$$

The overall thermal balance can be written as:

$$m_{storage} c_{sw} \frac{dT_{storage}}{dt} = Q_{coll} - Q_{loss} - Q_{toMD} \quad (2.26)$$

The blocks in the subsystem are shown in Figure 2.9.

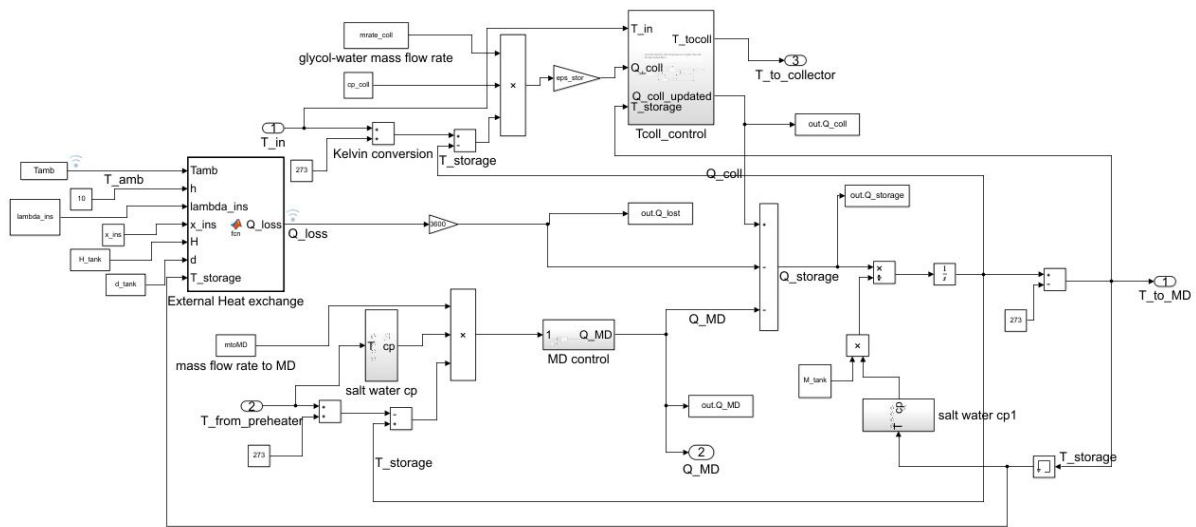


Figure 2.9: Blocks in the Storage Subsystem

2.6 Auxiliaries subsystem

The purpose of this subsystem is to guarantee a minimum inlet temperature to the MD unit. In particular, to provide a correct functioning of the system, an outlet temperature from the MD unit of minimum 40°C must be always assured. The logic contained in the program allows to trigger this subsystem, only when the temperature of the seawater contained in the storage is lower than the minimum value of inlet temperature, necessary to assure the previous condition. The heat delivered by the system to the water flowing, can be written as:

$$Q_{aux} = m_{toMD} c_{sw} (T_{min} - T_{storage}) \quad (2.27)$$

The evaluation of this quantity is important for the computation of the Solar Fraction (SF), necessary to view the plant's performances.

The subsystem works by means of a Proportional Integral (**PI**) Programmable Logic Controller (**PLC**), working with a feedback signal and contained in a specific Simulink block. This feedback signal is precisely the outlet temperature of the feed flow, which is compared with the assigned value in order to retrieve an error signal, directly sent to the PI. Lastly, this block gives as output a temperature signal compared with the temperature existing in the storage tank, so to decide whether or not to activate the auxiliaries. In Figure 2.10 is shown the previous logic.

An existing component chosen for this application is the aguaFLOW exclusive VPM 20/25 W, manufactured by Vaillant [40].

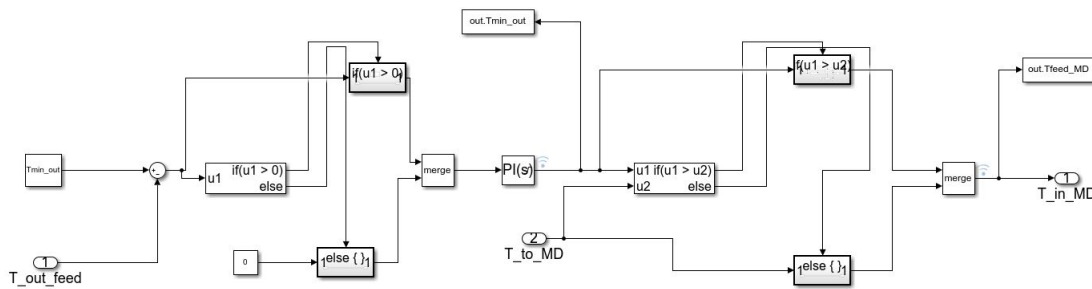


Figure 2.10: Auxiliaries subsystem blocks

2.7 MD subsystem

It has the purpose of simulating the functioning of a Membrane Distillation unit, capable of producing freshwater starting from seawater. The main component of this device is the microporous hydrophobic membrane, which allows the passage of vapour flux, but not of water and salt. The water vapour is generated by the heat provided to the flowing fluid, and is guided by an existing temperature gradient between the seawater flow (feed side) and the freshwater flow (permeate side).

The amount of fresh water produced is:

$$J = K \Delta p_v \quad (2.28)$$

where J [$kg/(sm^2)$] is the fresh water mass flow per unit area of the membrane, K [$kg/(sm^2Pa)$] is the membrane permeability and Δp_v [Pa] is the vapour pressure difference. The main characteristics of this technology are better explained in Subsection 1.4.4.

The permeability of the membrane depends mainly on two coefficients, namely:

1. **Knudsen diffusion**, relevant when the pore sizes are small. The coefficient can be expressed as:

$$K_{knudsen} = \frac{2\pi}{3RT} \left(\frac{8RT}{\pi M_w} \right)^{0.5} \frac{r^3}{\tau d_m} \quad (2.29)$$

where: $R = 8.314 [J/(molK)]$, $M_w [kg/mol]$ is the water molar mass, $r [m]$ is the pore mean radius, τ the tortuosity and $d_m [m]$ the membrane thickness;

2. **Diffusion in air**, can be expressed as:

$$K_D = \frac{\pi P D r^2}{RT p_a \tau d_m} \quad (2.30)$$

where: $p_a [Pa]$ is the air pressure in the pore, $D [m^2/s]$ is the diffusion coefficient and $P [Pa]$ is the partial pressure of water vapour;

The total permeability can be evaluated as:

$$\frac{1}{K} = \frac{1}{K_{knudsen}} + \frac{1}{K_D} \quad (2.31)$$

In this type of unit, this last will be considered independent from temperature, and so constant in time. The chosen membrane is the Aquastill [41], with the following characteristics:

Aquastill Membrane Data	
Thickness [μ m]	77
Porosity [%]	83
Average pore diameter [μ m]	0.2

Table 2.6: Membrane data

Thanks to some suitable correlations it is possible to calculate the value of the permeability, which is equal to $14.5 \times 10^{-7} [kg/(sPa m^2)]$.

To increase the productivity, the vapour pressure difference must be maximized. This can be done by maximizing the temperature gradient present between the permeate and feed side of the unit. Indeed, it is known by several laws (i.e Antoine's law) that the vapour pressure increases exponentially as the temperature increases. Consequently, it is important to calculate the heat transfer, in order to evaluate the temperatures and so the partial pressures.

Three thermal contributes can be identified:

1. Convection heat transfer between the feed side water flow and the membrane;

2. Conduction heat transfer and latent heat vapour mass transfer across the membrane;
3. Convection heat transfer between the permeate side water flow and the membrane;

The first can be expressed as:

$$q_{feed} = h_{feed}(T_{feed} - T_{m1}) \quad (2.32)$$

where: q_{feed} [W/m^2] is the thermal heat per unit area, h_{feed} [$W/(m^2K)$] is the convective heat transfer coefficient of the feed side, T_{feed} and T_{m1} [K] are respectively the feed fluid and membrane on the feed side temperatures.

The second can be calculated as:

$$q_{mem} = J\Delta H_v + \frac{k_m}{d_m}(T_{m2} - T_{m1}) \quad (2.33)$$

where: ΔH_v [J/kg] is the latent heat of water, $k_m = 0.27$ [$W/(mK)$] is the membrane thermal conductivity, and T_{m2} [K] is the membrane surface temperature on the permeate side.

Lastly the third contribute can be evaluated through equation:

$$q_{permeate} = h_{permeate}(T_{m2} - T_{permeate}) \quad (2.34)$$

Expressing the equations in function of T_{m1} and T_{m2} and calling $\frac{k_m}{d_m}$ as C_m :

$$T_{m1} = \frac{C_m(T_{permeate} + (\frac{h_{feed}}{h_{permeate}})T_{feed}) + h_{feed}T_{feed} - J\Delta H_v}{C_m + h_{feed}(1 + \frac{C_m}{h_{permeate}})} \quad (2.35)$$

$$T_{m2} = \frac{C_m(T_{feed} + (\frac{h_{permeate}}{h_{feed}})T_{permeate}) + h_{permeate}T_{permeate} - J\Delta H_v}{C_m + h_{permeate}(1 + \frac{C_m}{h_{feed}})} \quad (2.36)$$

It is possible to observe that the membrane temperatures are function of the fresh water mass flow rate. Indeed, in order to evaluate these three unknowns it is required an iterative procedure. In addition, the convective heat transfer coefficients are unknown, although, as described in Section 2.4, it is possible to retrieve these values from the Nusselt numbers. In case of laminar flow, the Graetz-Leveque equation has been used (Equation 2.37), contrarily in case of turbulent flow the Dittus-Boelter equation has been used (Equation 2.14).

$$Nu = 1.86(RePr\frac{d}{L})^{0.33} \quad (2.37)$$

At last, it is important to determine the outlet temperature of the feed side brine, in order to provide: the feedback to the Auxiliaries subsystem (see Section 2.6) and the inlet temperature signal to the Pre-heater subsystem (see Section 2.8).

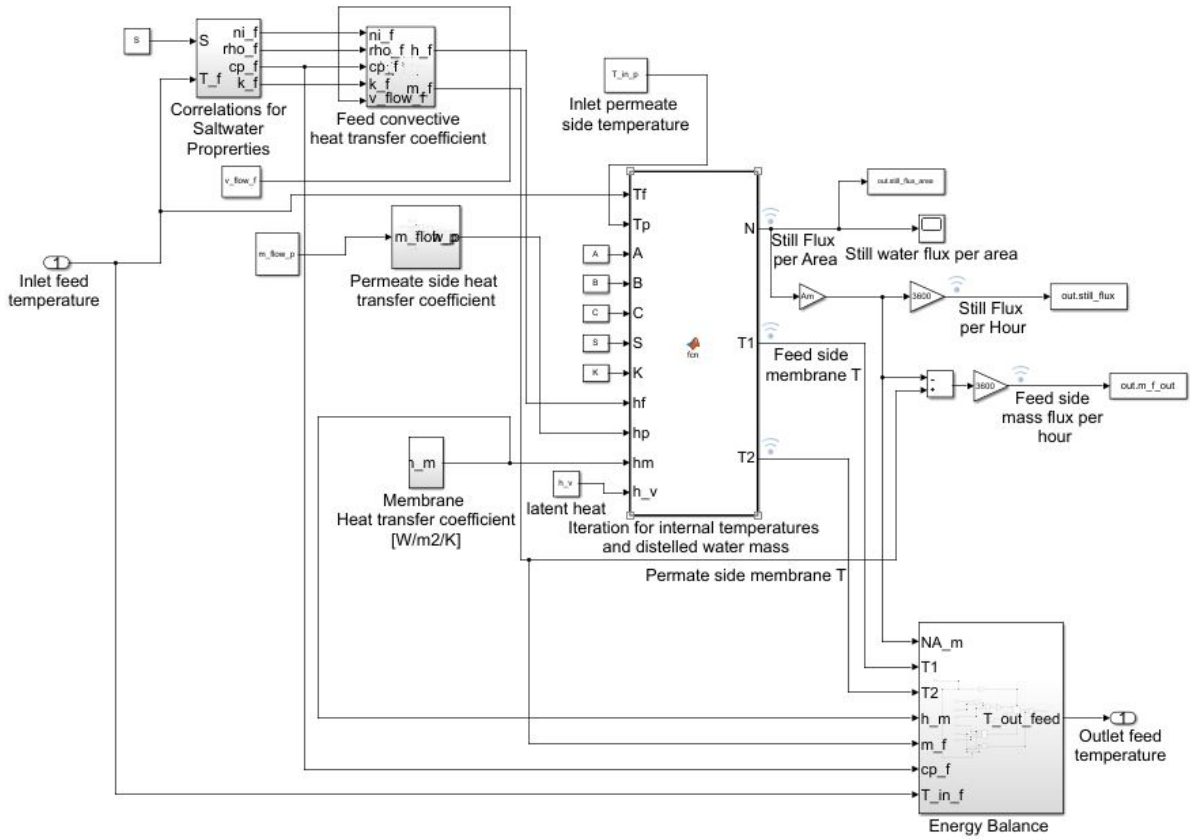


Figure 2.11: MD unit subsystem blocks

To evaluate this unknown, it is possible to write the thermal balance to the feed side closed volume:

$$\dot{m}_{toMDC_{sw}}(T_{feed} - T_{out,feed}) = JA_m \Delta H_v + C_m A_m (T_{m1} - T_{m2}) + Q_{lost} \quad (2.38)$$

where: $A_m [m^2]$ is the membrane area and $Q_{lost} [W]$ is the lost heat. This last can be evaluated by means of an empirical equation [42]:

$$Q_{lost} = -780.0180 + 33.1084 T \quad (2.39)$$

The internal blocks of the subsystem are shown in Figure 2.11.

2.8 Pre-heater subsystem

The main purpose of this subsystem is to simulate the functioning of a plate heat exchanger, required to: recover the latent heat of the outlet feed water and to allow the substitution of the discharged brine with pre-heated new seawater.

The device used is the same than the one considered in Section 2.5. As already said, in order to evaluate the temperature of the outlet new seawater is necessary to execute an $\epsilon - NTU$ analysis.

The key parameters of this method are:

- **NTU**, or Number of Transfer Units, defined as:

$$NTU = \frac{UA}{\dot{C}_{min}} \quad (2.40)$$

where: U [$W/(m^2K)$] is the global heat transfer coefficient, A [m^2] is the heat exchanger area and \dot{C}_{min} [W/K] is the minimum heat capacity rate, defined as:

$$\dot{C} = \dot{m}c \quad (2.41)$$

- ϵ , or thermal efficiency, defined as.

$$\epsilon = \frac{\dot{Q}}{\dot{Q}_{max}} \quad (2.42)$$

- r , which represents the ratio between the minimum and the maximum heat capacity:

$$r = \frac{\dot{C}_{min}}{\dot{C}_{max}} \quad (2.43)$$

Of all the previous parameters only ϵ is unknown, in fact UA is given by the manufacturer [39] (~ 323 [W/K]) and the heat capacities are easily calculable. In literature are present several equations which relate these three parameters, in particular:

$$\epsilon = \frac{1 - e^{-NTU+rNTU}}{1 - re^{-NTU+rNTU}} \quad (2.44)$$

Once known the thermal efficiency, it is possible to obtain the transferred heat (see Equation 2.22) and by means of the thermal balance, it is possible to derive the outlet temperature of the new seawater. In Figure 2.12 are represented the blocks contained in the subsystem.

3. Passive technology: A low cost solution for desalination

One of the biggest problems concerning passive devices is the waste of latent heat, released during the condensation of water vapour. Because of this, the thermal efficiency of the component, and consequently the water production are reduced. The *SMall Laboratory*, research group at Politecnico di Torino, overcame this problem by the realization of a multi-stage device, capable of retrieving the latent heat from a previous stage to generate new fresh water [43]. The purpose of this work is to develop an optimized version of this device, working with the same principle.

Due to the reduced dimensions of the new device, it has been chosen a modular configuration, allowing to decide the overall fresh water production simply varying the amount of devices. In the end all of these devices have been stocked in specific designed cases.

In the next sections it will be discussed: the working principle, the experimental configuration and the obtained results of the cited prototype.

3.1 Working principle

The main idea that drives the working principle of the device, is the reduced characteristic distance between the two hydrophilic layers, which allows an efficient multiple evaporation/condensation process. In Figure 3.1a is shown the mechanism driving the desalination process of a 3-stage prototype.

Every stage is composed of two hydrophilic layers and an hydrophobic membrane. The upper layer is the evaporator (where seawater is collected), meanwhile the lower one is the condenser (where the fresh water is collected) of the stage. These two are glued to the aluminum plates, except for some protruding strips which are respectively dripped in seawater and freshwater basins.

The device is passive since it is stand-alone, and doesn't need any external auxiliary system in order to operate. In fact, the water flux is driven exclusively by capillarity forces (given by the hydrophilicity of the layers) and gravity (due to the fact that the device is slightly inclined).

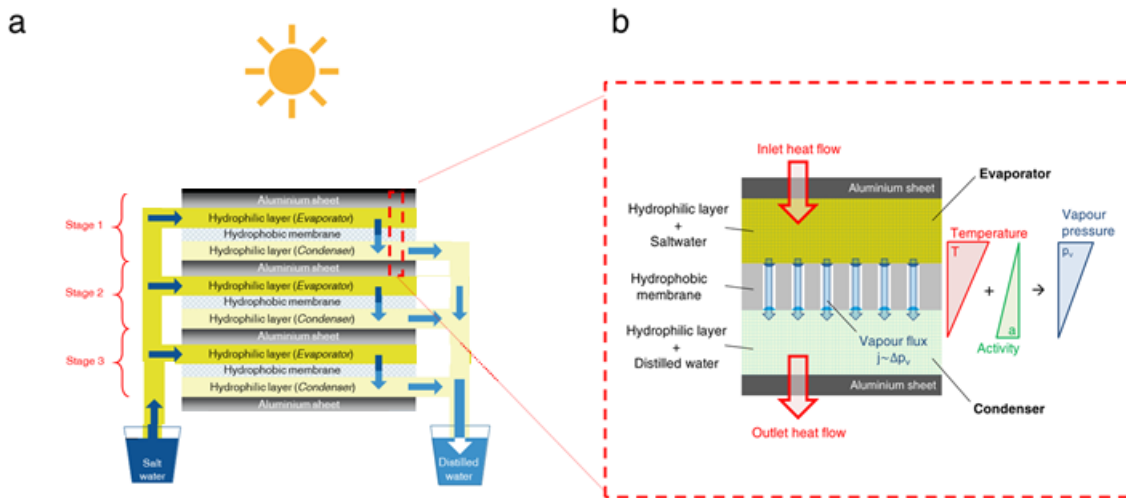


Figure 3.1: (a) Schematic of the 3-stage distillation device (b) Detail of a single stage of distillation, showing the temperature, the activity (i.e. salinity) and the vapour pressure gradients [43]

While working, the seawater rises along the evaporator of each stage thanks to capillarity. A thermal gradient is introduced between the top and bottom of the device by solar radiation, that hits the top absorbent surface. Due to this gradient, the upper aluminum plate evaporates the water contained in the evaporator, generating a vapour flux passing through the middle membrane. This flux is driven by the pre-existing temperature and activity gradients present in each stage (Figure 3.1). Then the vapour condenses in the lower hydrophilic layer, and drops in the basin (thanks to gravity) when saturation is reached. Finally, the latent heat of condensation is used by the undergoing stage to trigger evaporation, and so on for all the stages. As a result, the recover of latent heat allows the unit to have a high thermal efficiency, overcoming the typical limitations of passive devices.

In conclusion, it is worth to notice that differently from common solar sill technologies, where the condensation affects the optical transmittance of the device, here the performances are influenced exclusively by the solar irradiation available.

3.2 OHDC (Oman Humanitarian Desalination Challenge)

The guidelines for the design of the prototype have been given by an innovative world wide challenge named, *Oman Humanitarian Desalination Challenge*. Initiated by the MEDRC Water Research and the Oman Research Council, this challenge aims to find a new portable type of device, capable of providing a certain amount of drinkable water

in arid remote areas, or in critical scenarios. It's not surprising that a country as Oman initiated this campaign for water desalination, in fact according to the World Resource Institute, this region is ranked 16th in the world in terms of water scarcity [44].



Figure 3.2: Logo of the challenge [45]

In detail, there are seven principle restrictions for the realization of the prototype. These points will be used to decree the goodness or badness of the realized device, namely:

- **Low Cost** - Maybe the most restrictive obligation. Limits the cost of the device to a maximum of 20\$, in order to enhance the large scale production especially in the poorest areas;
- **Handheld-size** - The proposed device needs to be lightweight and small, since it might be moved by a single person day by day, or used for rescue purposes;
- **Short term use** - The device must be capable of working for a minimum of 30 days, without the necessity of a big maintenance;
- **Robust** - The apparatus must be resilient, and especially corrosion resistant. In fact, it should be capable of being employed in adverse situations without the risk of damaging or loosing some components (i.e bolts, cables);
- **Minimum rate of production** - The prototype must be able of producing a minimum of 3 liter/day even in cloudy conditions. This amount is a little more than the average daily necessity of a human being to survive;
- **Water Quality** - Starting from water 100 NTU (Nephelometric Turbidity Unit) containing 35 grL^{-1} , the apparatus must give as output water with a maximum of 1 grL^{-1} TDS. This threshold is given so to meet the WHO maximum contamination levels [46];
- **Stand-alone** - The device must be passive, so no external auxiliary systems or chemicals are allowed to be used in order to provide the correct functioning;

In conclusion, it has been decided to participate at this contest in order to elaborate a device that: has appealing for the main societies, respects the state-of-art solutions and receives constructive feedbacks from the scientific community.

3.3 Experimental set-up

In this section the main characteristics of the new prototype will be deeply analysed. It follows a description of the components needed to produce the device, along with their fabrication and assembling. Then, a description of the experimental layout will be examined. At last, the main features of the prototype will be discussed.

3.3.1 Composition

Once known the working principle of the device, it's optimization mainly concerned in: obtaining a modular configuration reducing the dimensions of the single device (and so increasing the transportability), substituting some components to reduce the overall complexity and cost (holding constant or increasing the productivity) and modifying some characteristics of the water supply in order to enhance the thermal efficiency.

In detail are here reported the components used for the realization of one panel (case with inserts for containing four devices):

- **Hydrophilic layers:** made of microfiber, bought with dimensions of 35x35 cm each (Figure 3.3c);
- **Hydrophobic layers:** made of polytetrafluorethylene (PTFE), bought with dimensions of 63x52 cm each and with pore size ranging between 0.1 μm and 3 μm (Figure 3.3d);
- **Aluminum sheets:** wholesale bought with thickness of 1 mm, cut by means of a jigsaw (Figure 3.3a);
- **Transparent plastic:** PMMA panels 1 cm thick, used to create the supports for the devices in the plastic case (Figure 3.12f);
- **Plastic components:** polypropylene (PP) used to shield the protruding strips of the layers, in order to prevent the free evaporation of water when exposed to direct sun irradiation. It has been sealed by means of a sealing machine;
- **Adhesive aluminum tape:** cut in strips and partially overlapped, to form a unique sheet, to further cover the protruding strips from solar irradiation (Figure 3.3b);

- **Seawater basin / Case:** polypropylene (PP) rectangular case of dimensions 60x40x7 cm, used to collect both four devices and the seawater (Figure 3.3e);
- **Fresh water gathering bag:** a catheter, cut at one end and appropriately glued in order to collect all the protruding strips of the condensers. One for each device is needed (Figure 3.3g);



(a) Aluminum sheets



(b) Adhesive aluminum tape



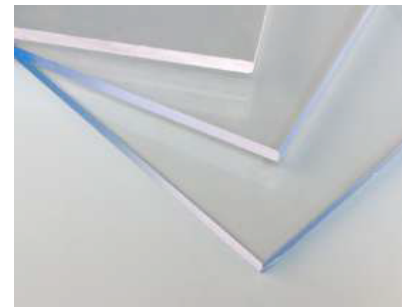
(c) Hydrophilic layer



(d) Hydrophobic layer



(e) PP case with installed the transparent plastic inserts



(f) Transparent plastic



(g) Catheter

Figure 3.3: All the components necessary for the realization of a panel

All the components are represented in Figure 3.3.

As a first step all the raw materials have been cut, in order to achieve the correct dimensions for the device, which are here reported:

- **Evaporator:** rectangle of dimensions 23x27cm;

- **Aluminum foils:** rectangle of dimensions 27x9cm;
- **Condenser:** rectangle of dimensions 37x7cm;
- **Membrane:** rectangle of dimensions 30x12cm;
- **Plastic supports:** rectangular trapezoid with length of 27cm, left height of 7cm and right height of 6 cm;



Figure 3.4: MACOM VAC2060

The hydrophobic, hydrophilic layers and the plastic components have been cut by means of precision cutters and scissors, meanwhile the aluminum and the transparent plastic with a jigsaw. The solar absorber instead is simply an aluminum foil, coated with a black pigmented paint, so to enhance the solar radiation absorption. At last, the plastic parts have been sealed together by means of a MACOM VAC2060 sealing machine (Figure 3.4).

It is possible to notice the simplicity of the geometries and the reduced dimensions for a single productive device.

vice.

Since the device is composed of 5 stages the total amount of pieces required are: 7 aluminum foils (one is the solar absorber), 5 evaporators, 5 condensers, 10 rectangular sealing plastic covers, 1 catheter and 5 membranes.

3.3.2 Assemble

Once all the components are known and available, it is possible to move to the assembling phase. No particular actions are required (except gluing and positioning), since the device is passive (stand-alone) and doesn't require any cables or chemical components.

It is possible to start from the assemble of the device, to pass then to the assemble of the case and then the final panel. Due to the fact that: the device is multi-stage and has no mechanical junctions, the assemble of the device consists exclusively in overlapping the different layers in the correct order.

At first, the condensers had been glued to one side of the aluminum foils distant 1 cm from both the superior and lateral edges of this last, as shown in Figure 3.5c. Then the plastic envelopes, previously sealed, have been inserted at the lateral sides of the evaporators measuring 25 cm. These last, were inserted deep enough to cover the protruding strips, but not to much, so to leave the highest amount of disposable working area (Figure 3.5b). Next, also this assemble has been glued to one side of the aluminum foils. Considering the

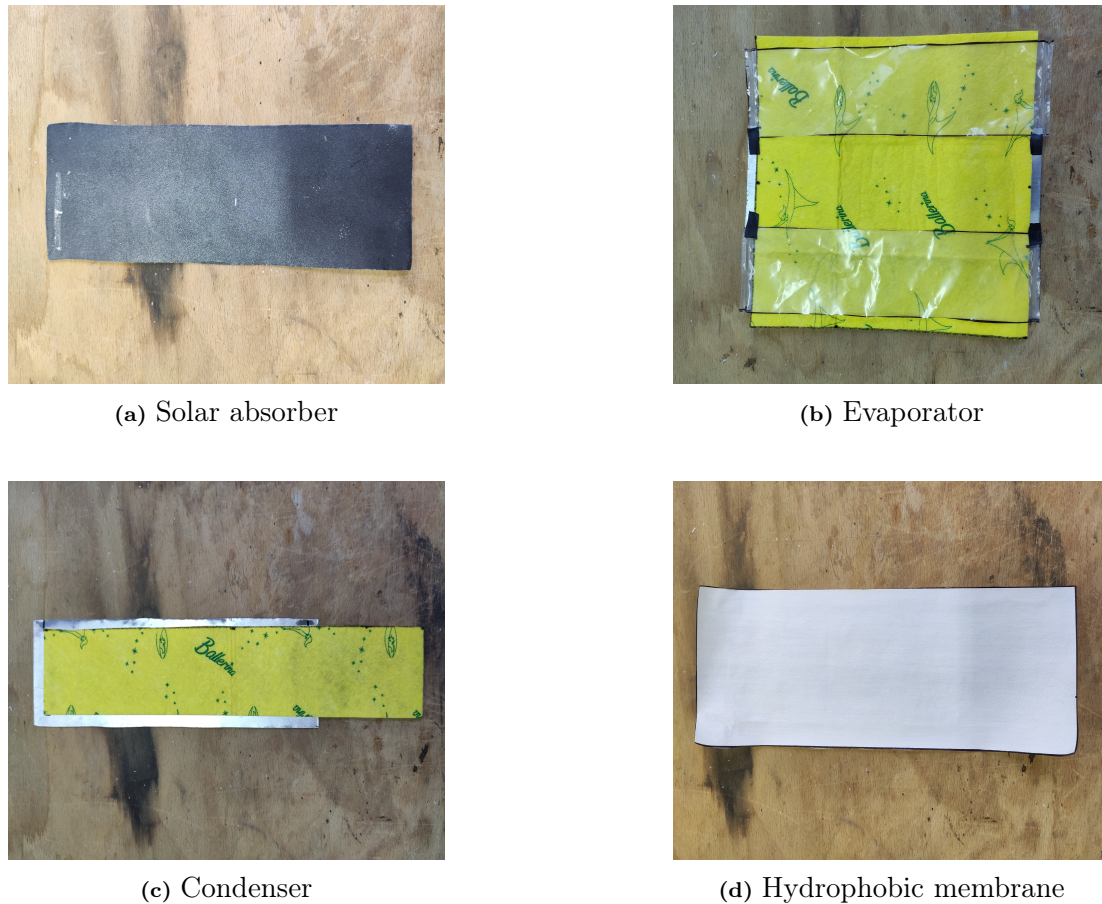


Figure 3.5: Different layers of the device

fact that, the device contains 5 stages, 4 foils will share an evaporator and a condenser, meanwhile 2 will have exclusively one of the two.

Once concluded this step, it is possible to overlap the layers, in order to produce the stratigraphy (Figure 3.6) of our device. The order to follow is this:

1. Aluminum foil with only condenser;
2. Membrane, with PTFE side (Figure 3.5d) facing towards the evaporator;
3. Aluminum foil sharing both evaporator and condenser, with the first facing the membrane;
4. Repeat points 2 and 3, until only the foil with the evaporator is remaining. The last visible surface should be a plane side of aluminum;
5. Place the solar absorber (Figure 3.5a) on the last surface, in order to enhance conductive heat transfer;

At the same way as illustrated before, it is possible to build how many devices required.

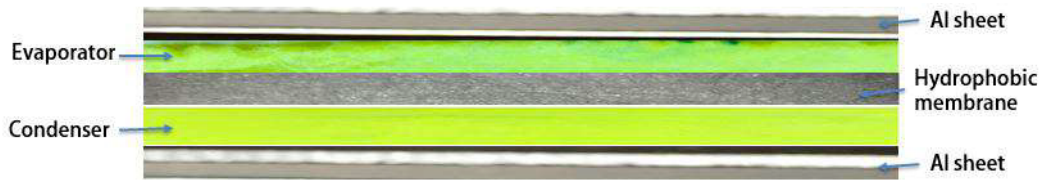


Figure 3.6: Stratigraphy of one stage

Once obtained the devices, it is possible to assemble the case that will hold 4 devices, generating a producing panel. The rectangular container can be shopped online by many wholesale sites (i.e Amazon, Alibaba), taking care of having the required dimensions of 60x40x7cm. The one used in these applications is a typical dough container used in many restaurants.

Owning the container, in order to produce the holders for the devices, the trapezoidal transparent plastic pieces have been glued (with hot glue or silicon) adjacent to one of the long sides of the case, taking care of pointing the inclined surface towards the outside of the box. This last appointment is important, so to enhance the flow of water from the condenser to the outside of the case, where the catheters will be installed. These supports must be glued at a distance of 5 cm from the 40 cm side of the basin, with an internal spacing of 9 cm and external spacing of 5 cm. Considering Figure 3.7, it is possible to observe the different subdivisions obtained once finished. The red slots (from 1 to 4) represent the areas occupied by the devices, meanwhile the blue areas (identified as 5) will be filled with salt water. Lastly, finished the previous tasks it is possible to assemble the final panel.

The devices must be placed on the transparent plastic supports, so to: cover the highlighted zones (1, 2, 3 and 4 of Figure 3.7), place the condenser's protruding strips outside of the white case and insert the evaporator's protruding strips in the middle slots, where seawater will be contained.

Finally, the pre-cut catheter can be attached to the solar absorber and bottom aluminum foil, in order to collect all the condensers of the device. The final result is shown in Figure 3.8, where only 2 devices are disposed.

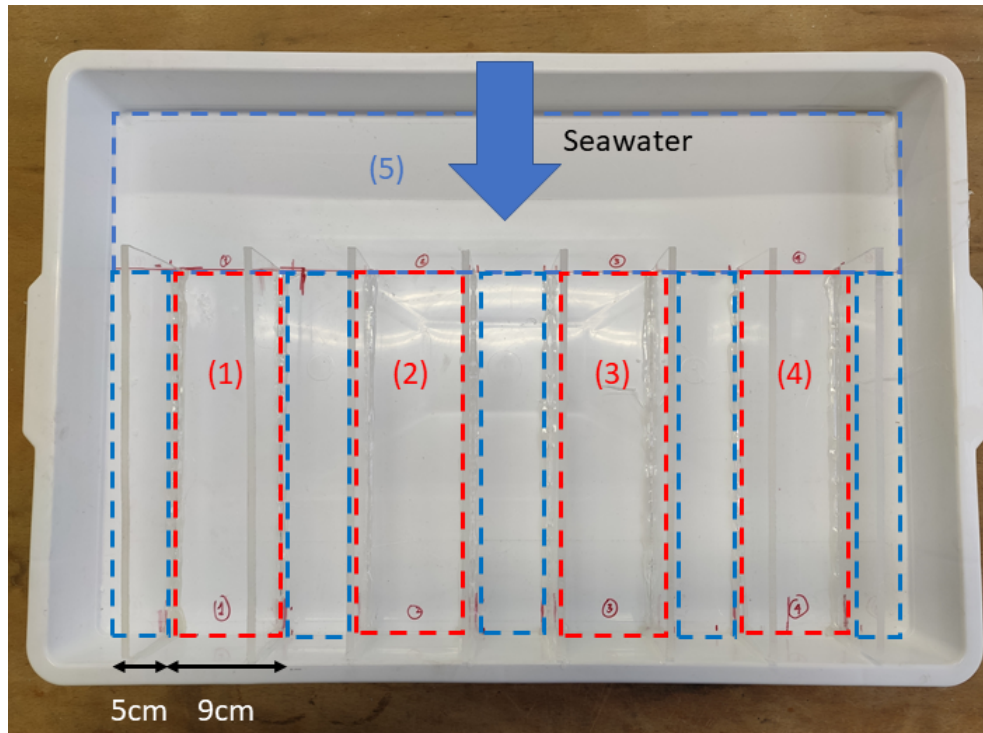


Figure 3.7: Subdivision of the case areas once the transparent holders are glued.



(a) Front view



(b) Upper view

Figure 3.8: Case with 2 devices and catheters installed

3.3.3 Features and characteristics

As previously discussed, all the design process undergone the criteria imposed by the OHDC, not only to join the challenge, but also to assure the device's appealingness. In this section the different impositions will be discussed, and in particular it will be exposed how the device meets these requirements.

Low Cost

Since the device works by means of a passive technology, the operating costs are negligible. The only expenses regarding this voice may be the manpower to: cut the raw material,

glue the components, fill the saltwater basin, transport and assemble the panels. However, these last operations are not much time consuming and do not require particular skills, so their cost will be neglected. Therefore, the panel's cost derives exclusively from the price of the different raw materials. These last, have been taken from the wholesale site named *Alibaba*, considering large orders. The final calculations are shown in Table 3.1, noticing that some prices are referred to m^2 , kg or units of product sold.

	Unit cost	Amount	Actual cost	Reference
Hydrophilic fabric	1.5 \$/kg	0.24 kg	0.36 \$	Alibaba wholesale
Plastic envelope of fabric	0.6 \$/kg	0.03 kg	0.07 \$	Alibaba wholesale
Aluminum sheets	2.00 \$/m ²	0.68 m ²	1.36 \$	Alibaba wholesale
Membrane	1.00 \$/m ²	0.72 m ²	0.72 \$	Alibaba wholesale
Catheter	0.1 \$/unit	4 units	0.4 \$	Alibaba wholesale
Plastic case	0.6 \$/kg	1.8 kg	1.08 \$	Alibaba wholesale
Total cost of one desalination panel			3.99 \$	
Total cost of five desalination panels			19.95 \$	

Table 3.1: Table showing the cost of the materials for one and five desalination panels

It is noticeable that, the price of one single panel is < 3 \$ and of five units is < 20 \$ which is the limit imposed by the competition. As shown more lately in the text, five panels are more than sufficient to overcome the minimum daily distilled water production.

It is useful to remind that one single production panel contains 4 devices with the supports, and the seawater case. This to testimony the irrelevant cost of the single device, which ranges around ~ 1 \$.

Hand-held size

The overall dimensions of each desalination panel are 60x40x7cm and weights 3.2 kg (without seawater and with the dry devices).

All the devices are collected in panels, which can be easily piled up for being transported. In order to have the challenge desired productivity, five panels had to be considered (reaching a total of 16 kg). Furthermore, it has been considered the possibility to insert the panels in two ergonomic suitcases, equipped with handles to further improve the transportability of the total asset.

Robust

The device should be: resilient, corrosion resistant, have a long life and should minimize the use of spare parts that can be lost.

This requirement is necessary to allow the possibility of using the device in emergency conditions, or in particular harsh areas. The illustrated device is composed only of staked layers, so there are no moving part that can brake, no sealing that can leak and no wires that can fail. Furthermore, this configuration allows to confer resilience to the device, due to the fact that, any small damages or misalignment of the layers do not block the water production. The most delicate layer, namely the hydrophobic layer, is placed between two soft microfiber layers which prevent any tears and cuts.

The device skeleton is constituted by aluminum foils, which are well known for the corrosion resistance. This is because, when the aluminum initially oxidises generates an aluminum oxide coating, which protects the material from further corrosion.

Finally, when not used the device (in particular the microfiber) doesn't deteriorate and is always ready for working in emergency situations.

Short-term use

The device must operate for a minimum of 30 days, with low maintenance.

In the presented device the mechanical maintenance is nil, while the only necessary operations concerns in re-filling the seawater basin and collect the fresh water from the catheters, once in a while during the day. This great autonomy is given by the innovative geometry, which allows to: collect water from both the sides of the device (reducing dry-out effects and re-establishing the correct salinity of the device after few hours from the usage) and uses the Marangoni effect to control the salinity in the evaporator during operation [47].

During the tests, in order to avoid the transient phase given by the saturation of the condenser, this last has been initialized by wetting it with fresh water, before the solar exposure. This step has been done to reduce the test hours and to better measure the real production of the device. This lack of this step should not reduce the efficiency of the device, but more hours are required to achieve the same amount of fresh water.

Lastly, a continuous week of testing didn't evidence a particular degradation of the device and a significant reduction of the efficiency.

Rate of production



Figure 3.9: PV infinity ISOsun solar simulator

Due to impossibility of placing the device outside at real solar irradiation (the experimental campaign has been computed in September/October), the device has been tested indoor by means of a solar simulator, namely the *PV infinity ISOsun* shown in Figure 3.9.

This device is capable of providing a constant 1000 W/m^2 on a working area of $30 \times 30 \text{ cm}$, by means of the emission light of a lamp. Inside the device are installed some fans, which are needed for the lamp cooling, providing in our case a simulation of convection conditions present in external environments.

Starting from saltwater containing 35 g/L of salt, the whole desalination technology (made of 20 devices or 5 panels) has demonstrated to produce 1.78 L/kWh of distillate in average. This means that the whole asset provides 1.78 liters of distilled water (0 g/L), per each kWh of solar thermal energy. From experimental measures, the productivity ranged from 1.43 L/kWh (worst data collection) to 2.13 L/kWh (best data collection).

Considering the average solar irradiation of Muscat in September (i.e 199 kWh per squared meter per month [30]), considering the retrieved results, the whole desalination technology is able to produce in average 8.38 L/day of distilled water (6.74 L/day worst scenario; 10.03 L/day best scenario).

Considering that the challenge request is of 3 L/day , the 5 panels can fully satisfy the requirement. The excess of production can be stocked for cloudy days where no solar irradiation is present.

The modularity of the technology allows to assure always a certain amount of distilled water produced. For example, if one panel fails or damages, freshwater will be anyway produces by the other 4 panels, despite the reduction of $1/5$ of the productivity.

Stand-alone

As already specified the device is passive, namely it's working principle is based on thermal distillation (evaporation and condensation driven by thermal gradient), provided by solar irradiation. Indeed, there are no moving parts, no chemicals (no risk of contamination) or external materials.

The devices can work without any supervision during the day, in particular no sun tracking or solar concentration are present. The whole asset is made of simple components, easy to handle, difficult to loose and non dangerous for the operators.

Lastly, the assemble of a single 5 stage device can be done in one minute by a single person, once the order of the layers is fully understood.

Quality

Thermal distillation is well known for the capacity of reducing the salinity of water. During the experimental campaign almost every time the measured salinity has been of 0 g/L, reaching maximum values of 1 g/L, given by occasional contamination or instrumental errors. The salinity has been measured by means of a digital refractometer shown in Figures 3.10.

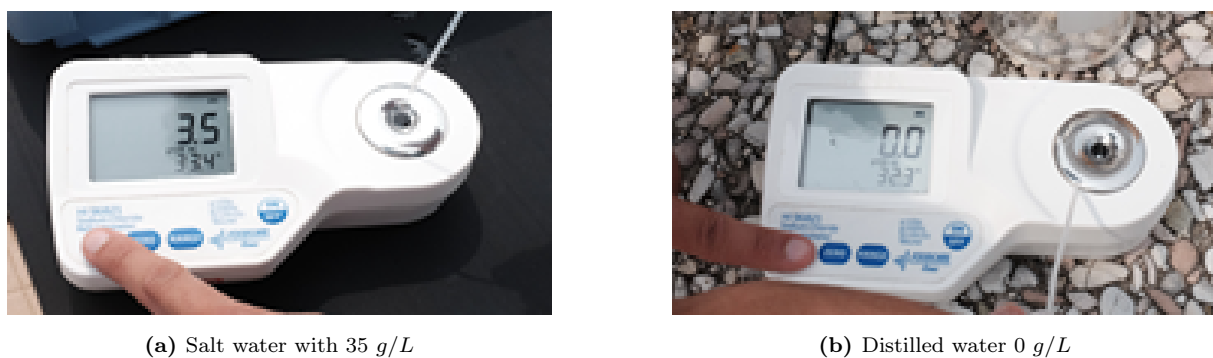


Figure 3.10: Salinity measurements by means of digital refractometer

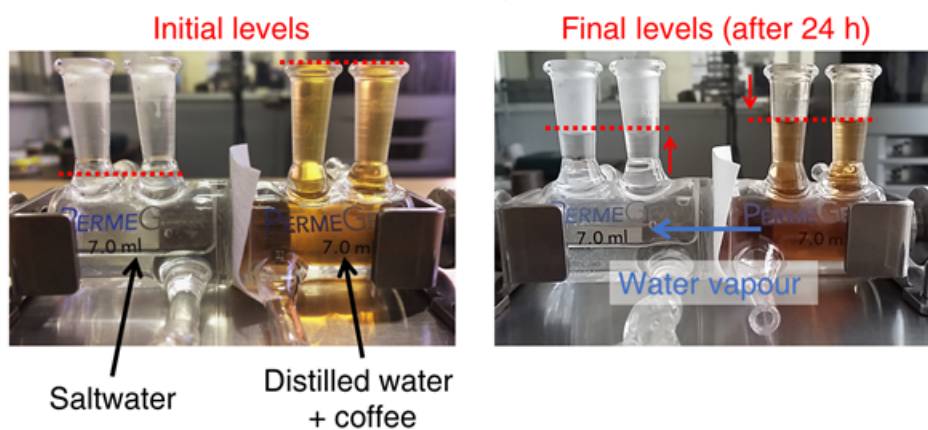


Figure 3.11: Initial levels of water and after 24 hours of contact. It is possible to observe the impossibility of the particles passage across the membrane

Furthermore, thanks to the presence of the membrane, particles contained in the inlet water are unable to pass. Hence, the input turbidity of the initial water doesn't affect the quality of the final distilled water. In Figure 3.11 is shown a test, which demonstrates the membrane's capacity of blocking the particles, also in concentrations of 100 NTU.

Lastly, thanks to the high temperatures reached during the distillation process, it is probable that most of the present bacteria perishes. This allows the potability of the provided the water, without any post-process treatments.

All the main features described in this section are verbally resumed and reported in a published video at the following link [Small OHDC video](#).

3.3.4 Experimental layout

As previously mentioned the majority of the experiments have been taken indoor, due to the seasonal lack of solar irradiance. This fact allowed to relate the production of water to a constant amount of solar radiation, namely 1000 W/m^2 , provided by the solar simulator. Contrarily, no real applications in an external environment could have been taken.

Do to the lack of time for the experimental campaign, no thermal analysis has been conducted on the device, but only a measure of water productivity. Despite this fact, it is plausible that the prototype proposed behaves thermally as the previous versions, considering also the change in the geometry. To confirm this fact, it is possible to observe the numerical simulations in the following chapter, and the superficial values of temperature reached on the solar absorber.

In conclusion are here illustrated the instrumentation needed for the experimental campaign taken on a single device:

- **Digital refractometer:** for salinity measurements;
- **Modular Distiller:** device under investigation;
- **Thermal gun:** needed for infrared measurement of superficial temperature of the solar absorber;
- **Digital scale:** for distillate water mass measurement;
- **Pipette:** to extract the water (salty or distilled);
- **PV infinity ISOsun:** sun simulator (see Figure 3.9);
- **Metallic support:** provided together with the solar simulator, allows to regulate the height of the device;
- **Seawater basins:** rectangular seawater basins adopted for a single device;

In Figure 3.12 are represented all the instruments.

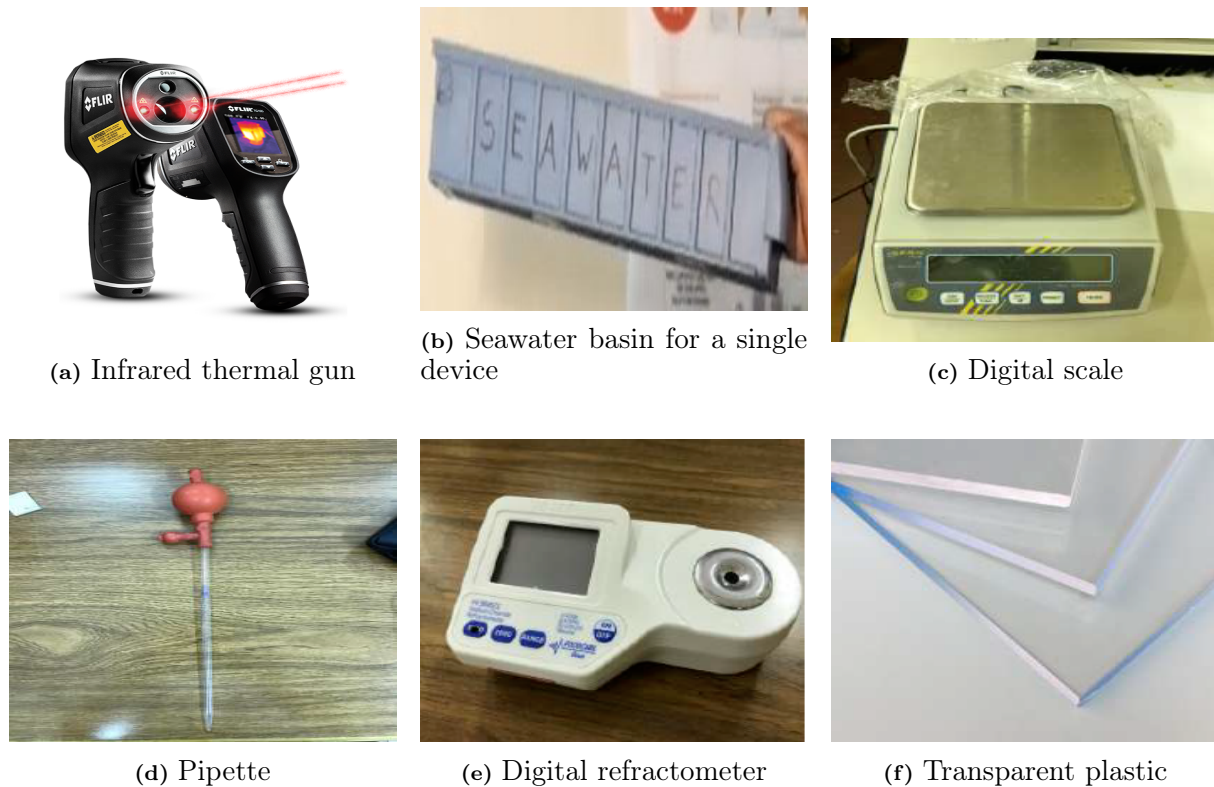


Figure 3.12: Different instrumentation necessary for the experimental campaign

At the beginning of the first day, the cleaned (with dry evaporator and condenser) device has been assembled, and placed on an slightly inclined surface. Then, the device has been initialized, by saturating the two layer respectively with salt water and fresh water, in order to reduce the unproductive initial transitory phase. Next, the two seawater basins have been filled with salt water (35 g/L) and placed at the sides of the device. The already wet protruding strips of the evaporator have been immersed in the saltwater in the basins, and the ones of the condenser have been collected in a single catheter. At last, all the apparatus has been placed on an adjustable steel platform, positioned underneath the solar simulator irradiated area.

Once initialized the apparatus, the experiment consisted in weighting and checking the salinity of the produced water every hour, for at least 5 hours. At the end of the productive day, the reached temperature of the solar absorber and the salinity along the axis of the evaporator has been measured and registered, leaving at the end of the procedure the device in the initial configuration (protruding strips of the evaporator immersed in salt water). The following day, the salinity of the evaporator has been measured again, to take track of the eventual salt diffusion hypothesized during design, and the condenser has been re-initialized, due to the fact that fresh water went away during the night by means of osmosis. Once done these two passages, the device was ready to be exposed to

solar irradiation, so the procedure previously exposed has been repeated.

In all this description, it is important to notice how the device requires almost no operational maintenance from one day to the other, increasing the resiliency and the facility of usage of the technology.

3.4 Theoretical model

To conclude this chapter, in this section will be exposed the theoretical model supporting the general system working principle. A good analysis of the physics behind this technology allows to better understand the pros and cons of the device and is necessary to implement the numerical simulations described in the following chapter.

The driving force of each stage is the vapour pressure difference existing between each evaporator and condenser. As already mentioned before, this latter is given by the difference in water activities (depending inversely to water salinity) and vapour pressures (directly proportional to temperature), present at the two sides of the hydrophobic membrane. The Raoult's law describes this effect:

$$\Delta p_v = a(Y_E)p_v(T_E) - a(Y_C)p_v(T_C) \quad (3.1)$$

where Δp_v [Pa] is the water vapour pressure difference, depending on: the temperatures T_E (evaporator) and T_C (condenser) [K] and the water activities a , depending on the salt mass fractions Y_E (evaporator) and Y_C (condenser).

It is important to better analyse the different components of the Raoult's law, starting from the water activity described in Equation 3.2 (considering ideal conditions).

$$a = \frac{M_{NaCl}(1 - Y)}{M_{NaCl}(1 - Y) + N_{ion}M_{H_2O}Y} \quad (3.2)$$

where M_{NaCl} (58.44 g/mol) and M_{H_2O} (18.02 g/mol) are respectively the molar masses of the sodium chloride and water, $N_{ion} = 2$ are the number of ions present in the sodium chloride molecules and Y ($m_{salt}/m_{solution}$) is the water salinity that can be computed both for the condenser and the evaporator. Considering the condenser ($m_{salt} = 0$ and $Y = 0$, dealing with fresh water) the water activity $a = 1$, meanwhile considering the evaporator ($m_{salt} = 0.035$ kg and $Y = 0.035$, dealing with sea water) $a = 0.978$.

Furthermore, in Equation 3.1 it is possible to notice that the water pressure itself influences the water pressure difference. This last can be historically estimated by several formula's, in this text the Antoine's semi-empirical correlation has been used, namely:

$$\log[p_v] = A - \frac{B}{C + T - 273.15} \quad (3.3)$$

where: p_v is the vapour pressure expressed in mmHg, A, B and C are material constants and T is the temperature expressed in Kelvin. It has a range of validity from 0.01 bar to 2 bar, large enough for the purposes of this text work. In this case of study, the material constants are respectively: $A = 8.07$, $B = 1730.63$ and $C = 233.42$ [48].

Once resumed these quantities, it is fundamental to analyse the analytical solution to derive the specific mass flow rate of freshwater (J), which indicates the productivity of our device. To do so, the same steps carried out by professor Chiavazzo [49] for the previous version of the device are here retraced. In this piece of literature the "Maxwell-Stefan model" and the "Dusty-Gas model" have been combined to derive a simplified equation for the specif mass produced. The first model, takes into account both the chemical potential and the molecular diffusion phenomena, generated by the total pressure gradient. The reasonable assumptions made are here listed:

- The mixture of water vapour, hydrogen and nitrogen is approximated with a binary mixture of water vapour and air;
- The air molar flux is considered nil, supposing the air molecules stuck in the membrane pores;
- Since the whole system works at ambient pressure, the viscous flow is considered nill;
- The gasses in the process are considered ideal. The chemical potential of water vapour is $\mu_w = \mu_{w,pure} + RT \ln[x_w]$, being: $\mu_{w,pure}$ pure water vapour chemical potential, R the ideal gas constant ($8.314 J/(K mol)$), T the temperature in Kelvin and x_w the water mole fraction;
- The water mole fraction can be assumed much smaller than one ($x_w \ll 1$), due to the fact that condensation happens downstream the pore, and not within the membrane where air is present;
- Pure Knudsen regime can be considered, when the pore size is small ($\sim 0.1 \mu m$). In fact, when the mean path of the molecules is comparable with the scale of the system (pores walls in this case).

Thanks to the previous considerations it is possible to approximate, through a 1st order Taylor series, the specific mass flow rate as:

$$J = K \Delta p_v \tag{3.4}$$

where $K [kg/(Pam^2s)]$ is the permeability coefficient of the gap present between the two hydrophilic layers. This last can be approximated as a sum of different contributions.

1. Interaction between vapour and vapour;
2. Interaction between vapour and pore wall;
3. Interaction between vapour and air present in the gap;

Namely, K can be calculated as:

$$\frac{1}{K} = \frac{1}{\frac{\epsilon_m P D_{wa} M_{H_2O}}{p_a \tau R T d_m}} + \frac{1}{\frac{2\epsilon_m r M_{H_2O}}{3RT d_m \tau} \sqrt{\frac{8RT}{\pi M_{H_2O}}}} + \frac{1}{\frac{P D_{wa} M_{H_2O}}{p_a R T d_{air}}} \quad (3.5)$$

where: ϵ_m is the membrane porosity, P is the total pressure, D_{wa} is the diffusion coefficient of water vapour in air, p_a is the arithmetic mean of the air partial pressure, τ is the tortuosity, d_m is the membrane thickness, d_{air} is the air layer thickness and r is the average pore radius of the membrane. Furthermore, for this application it is possible to estimate the product $P D_{wa}$ as:

$$P D_{wa} = 1.19 * 10^{-4} T^{1.75} \quad (3.6)$$

In addition the tortuosity can be evaluated by means of the Mackie-Maeres equation as below:

$$\tau = \frac{(2 - \epsilon_m)^2}{\epsilon_m} \quad (3.7)$$

All the previous equations have already been verified in the previous versions of the device, finding a good accordance with the numerical and experimental results.

At last, it is important to better analyse the specific flux present between the evaporator and the condenser during operation. This last can be evaluated considering the following equation:

$$q = \frac{k_{eff,g}}{d_{gap}} (T_E - T_C) + J \Delta h_{LV} + q_{lost} \quad (3.8)$$

where: $k_{eff,g}$ is the effective thermal conductivity within the eventual air gap and membrane, d_{gap} is the thickness of each stage. Δh_{LV} the enthalpy of vaporization and q_{lost} is the specific heat lost at the borders of the device's stages.

It is important to point out that the water flow in the hydrophilic layers is almost static, so the whole heat transfer process is mainly given by conduction (convection is negligible). All these considerations are fundamental to better understand the COMSOL simulations done in the next chapter.

4. Results

Once completely described the two desalination systems, the results obtained by the experimental campaign and the numerical simulations are here reported.

Considering the active plant, no experimental campaign has been conducted, so the unique available results are the numerical ones.

As far as the passive device is concerned, the numerical simulations have been performed by means of COMSOL Multiphysics software. These results will be compared with the experimental ones, retrieved in the Politecnico's laboratories, in order to validate or discharge the results obtained.

4.1 Active Plant

Simulations are exploited in order to maximize the solar fraction and the distillate annual production for the two types of collectors adopted. Specific parameters have been ranged between chosen values, so to completely describe the plant's behaviour in the different conditions. The limits have been imposed by the available components in the different wholesale shop and by the overall sizes of the plant, in particular:

Variable	Minimum	Mean	Maximum
ETC area [m^2]	2	12	24
Membrane area [m^2]	0,05	0,2	0,8
Storage tank volume [l]	150	500	1917
Outlet feed temperature [$^{\circ}C$]	40	50	60

Table 4.1: Chosen values for the different variables

By choosing the correct combination of these variables and holding constant the remaining data (i.e mass flow rate and solar data) it has been possible to identify for each technology the maximum and minimum of the solar fraction and distillate production.

In the next subsections are reported the results obtained for the two collector types selecting Turin as the desired location for the simulation.

4.1.1 Constant inputs

Here are illustrated the different input data which will remain constant during the simulations. The solar data, which consists of collectors disposition and solar irradiation are predetermined once chosen the geographical and installation locations. In this case Turin has been selected as city of interest and the collectors have been placed on a rooftop with a certain inclination. Figure 4.1 and Figure 4.2 give a first impression of the order of magnitude of the dealing irradiances. The maximum values range between 800 and 1000 W/m^2 in the summer season and the minimum is below 100 W/m^2 in the winter season.

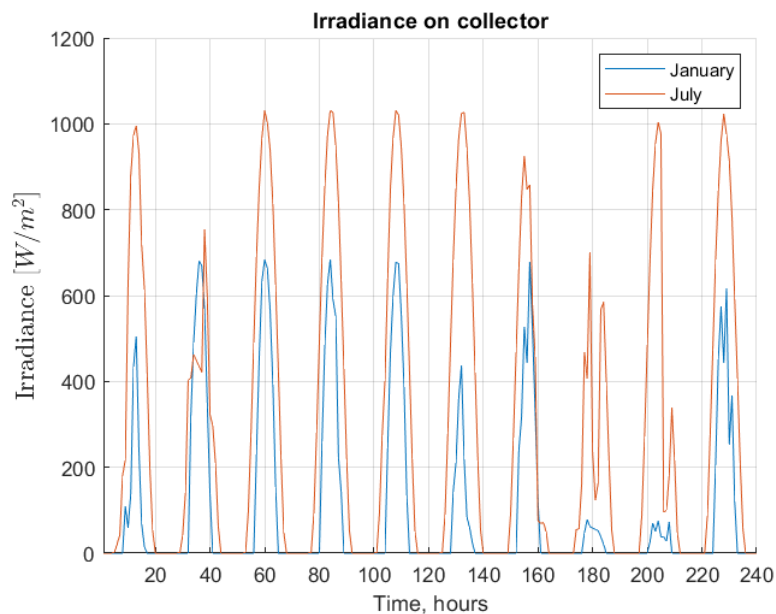


Figure 4.1: Irradiance per collector surface in the first ten days of January a July

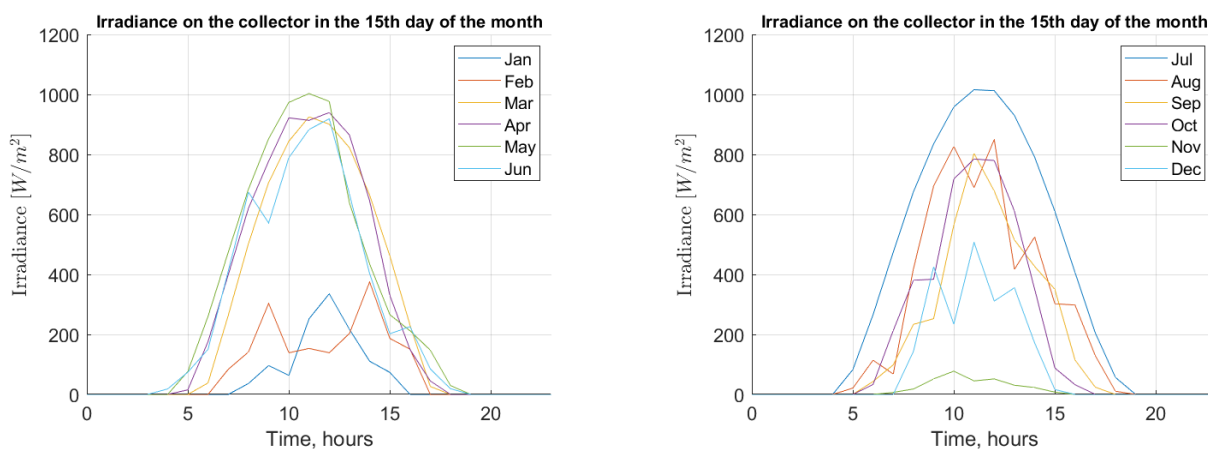


Figure 4.2: Irradiance on the 15th day of each month of the year

Other important parameters that have been set constant are: the mass flow rate evolving in the MD system, the inlet permeate temperature and the new seawater temperature. All the values assumed for these parameters are collected in Table 4.2.

Solar Data [°]	
Latitude, ϕ	45
Slope, β	25
Azimuth, γ	-22.5
Temperatures [°C]	
Inlet permeate	20
New seawater	20
Mass flow rate [kg/h]	
To MD system, m_{toMD}	100

Table 4.2: Constant input parameters

4.1.2 ETC collectors

In Table 4.3 are illustrated the different configurations considered and the corresponding results, in terms of annual distillate production and solar fraction.

ETC	1st	2nd	3rd	4th
ETC area [m^2]	24	24	24	24
Membrane area [m^2]	0.05	0.8	0.05	0.2
Storage volume [l]	500	150	1917	500
Outlet feed temperature [°C]	40	60	40	50
Results				
Solar Fraction [%]	90.31	20.87	44.16	50.1
Annual Water Production [$l/year$]	2551	35507	1235	8523
Annual Power Consumption [kWh]	15028	72609	72931	27596

Table 4.3: ETC configurations and corresponding results

From Figure 4.6 and 4.5 it is possible to justify the results obtained for the different configurations. Indeed, it is observable that to increase the solar fraction it is necessary to increase the mean storage temperature and reduce the required inlet feed temperature, so to reduce the auxiliary delivered heat and increase the heat storage capability of the

plant. Indeed, the solar fraction can be expressed as:

$$SF = \frac{Q_{sun}}{Q_{sun} + Q_{aux}} \quad (4.1)$$

The water production instead is largely enhanced by a bigger membrane surface and temperature difference between the feed and the permeate side. This latter can be only increased by increasing the inlet feed temperature, since the inlet permeate water is hypothesized constant.

From Figure 4.4 it can be concluded that the best configuration adoptable is the fourth, which allows a compromise between the solar fraction and the annual distillate production of the plant.

Considering the operational and capital expenditures of the plant (see Figure 4.3), the water price which allowed to reach the break even point in 30 years, considering the fourth configuration, is 0.3132 €/liter. In particular it has been considered the Net Present Value defined as :

$$NPV = \sum real\ cash\ flow = \sum discount\ rate \cdot cash\ flow \quad (4.2)$$

where the *discount rate* is a factor that converts the computed cash flow in a suitable value for the specific year and the *cash flow* is the money entering and exiting the company (i.e capital cost, operational cost and income). Fixed the plant life at 30 years, it is possible to determine the unitary cost of water which sets to zero the NPV in this amount of time.

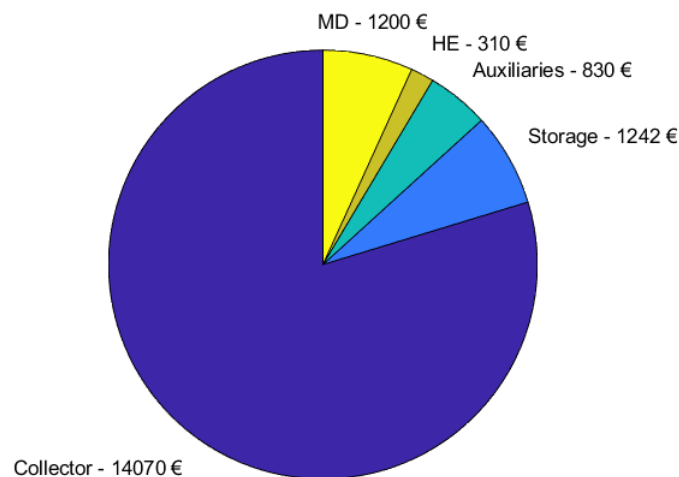


Figure 4.3: Capital cost of the different components

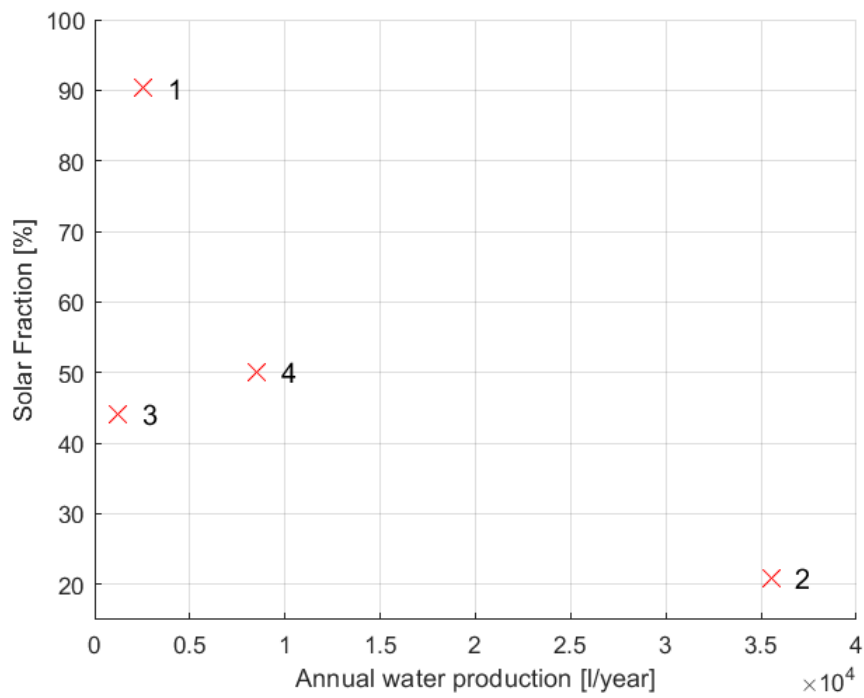


Figure 4.4: Scatter plot of the different configurations

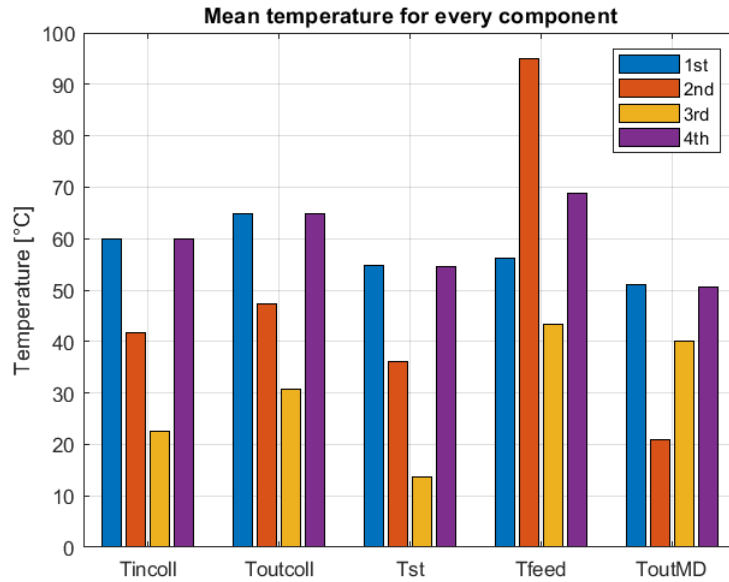


Figure 4.5: Annual mean temperatures of the fluids evolving in the different sections of the plant considering the different configurations

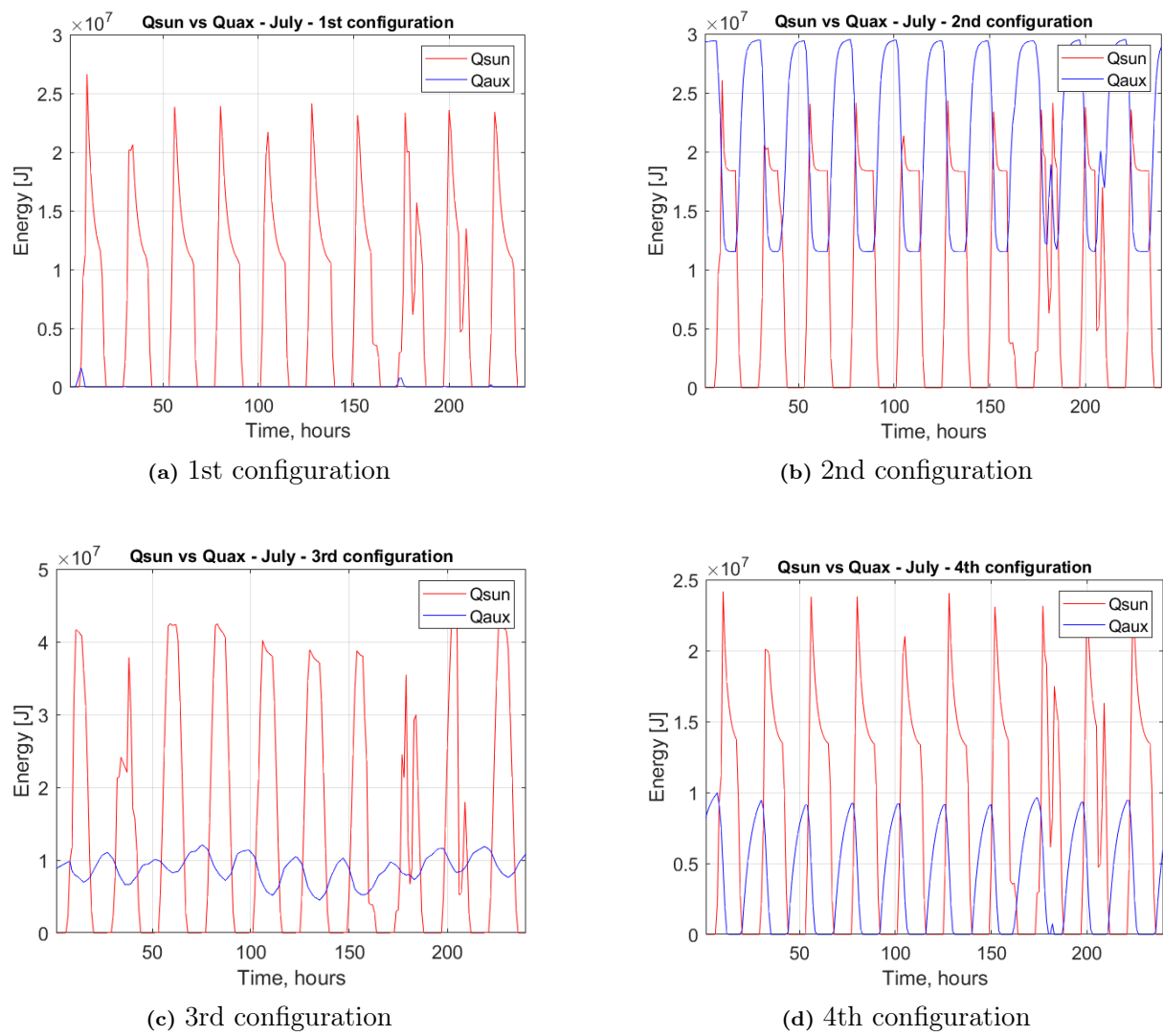


Figure 4.6: Heat delivered by the sun versus the heat provided by the auxiliary system

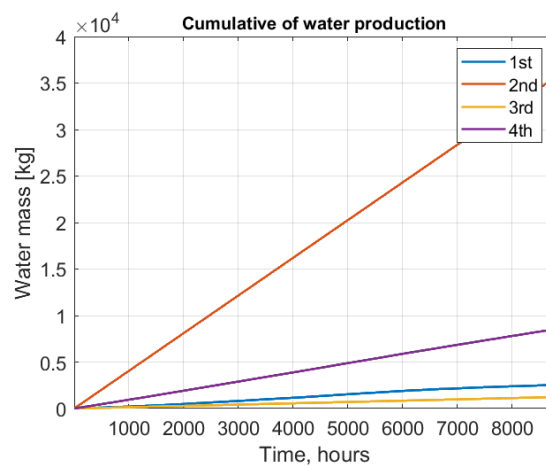


Figure 4.7: Annual distillate water production in the 4 configurations

4.1.3 PSC collectors

In Table 4.4 are illustrated the different configurations considered and the corresponding results, in terms of annual distillate production and solar fraction. All the consideration done in the ETC case are the same.

Considering the operational and capital expenditures of the plant (see Figure 4.8), the water price which allowed to reach the break even point in 30 years, considering the fourth configuration, is 0.3379 €/liter. The calculations solved are analogous to the ETC collectors case.

PSC	1st	2nd	3rd	4th
PSC area [m^2]	9.583	9.583	9.583	9.583
Membrane area [m^2]	0.05	0.8	0.05	0.2
Storage volume [l]	500	150	1917	500
Outlet feed temperature [$^{\circ}C$]	40	60	40	50
Results				
Solar Fracriion [%]	82.04	18.95	34.73	44.26
Annual Water Production [$l/year$]	2456	35507	1241	8082
Annual Power Consumption [kWh]	15452	73696	44221	29503

Table 4.4: PSC configurations and corresponding results

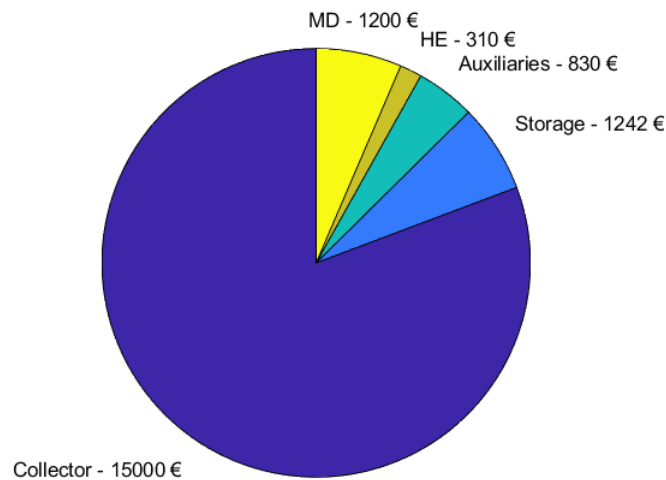


Figure 4.8: Capital cost of the different components

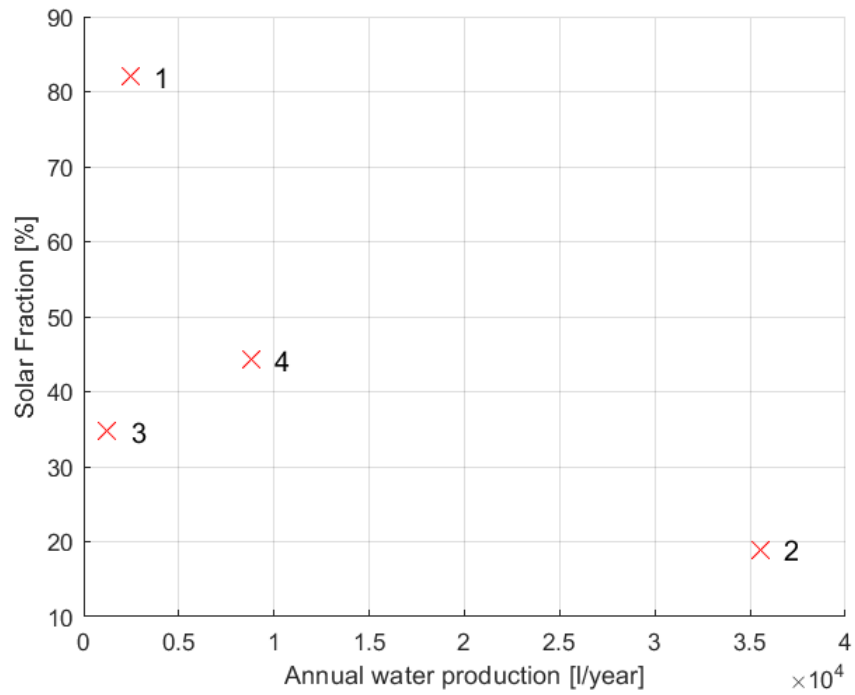


Figure 4.9: Scatter plot of the different configurations

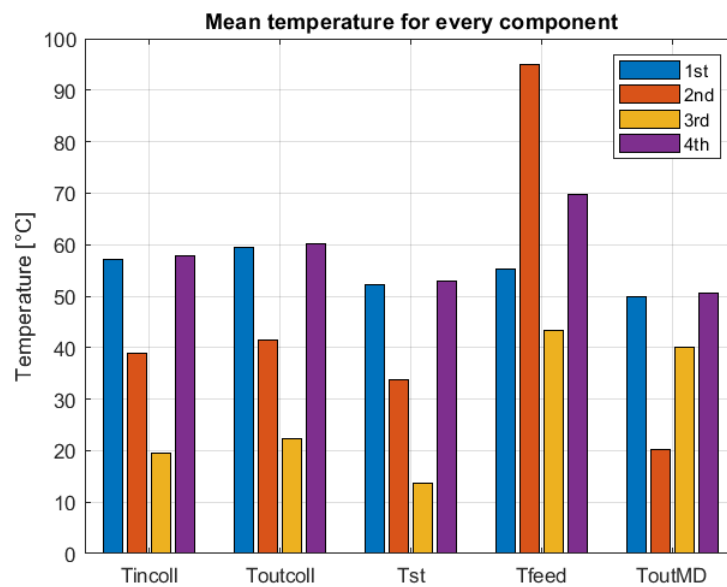


Figure 4.10: Annual mean temperatures of the fluids evolving in the different sections of the plant considering the different configurations

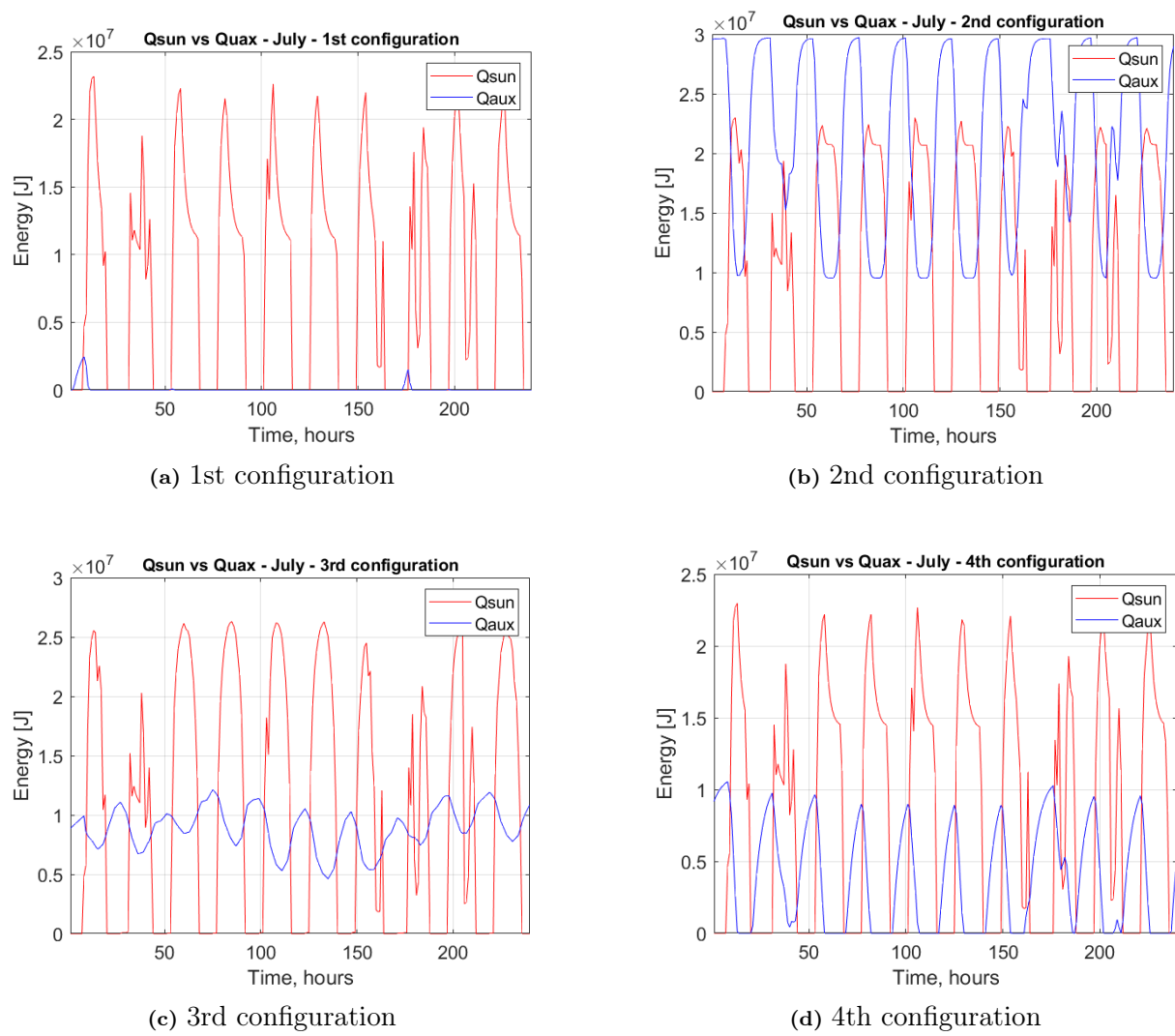


Figure 4.11: Heat delivered by the sun versus the heat provided by the auxiliary system

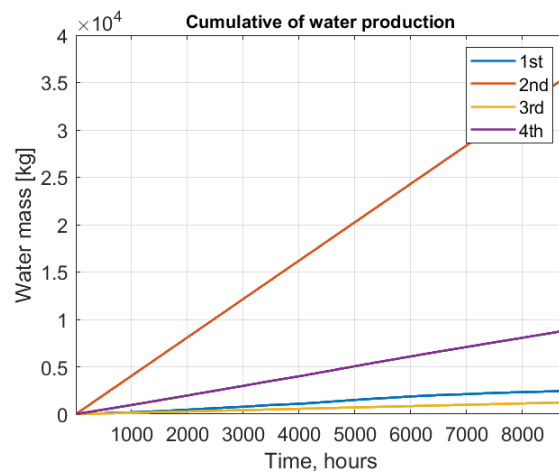


Figure 4.12: Annual distillate water production in the 4 configurations

4.1.4 Summary

From both the technologies it is possible to observe the limited capability of the designed plant based on MD. The low production of water can be mainly attributed to the MD subsystem and in particular considering that:

- MD technology is still a developing technology;
- The dimensions of the membrane are limited. Indeed, the module used is a laboratory one and its dimensions are directly proportional to the water production;

Also the elevated cost of the water is strictly related to the poor performances of the plant, since the productivity is not capable of rapidly overcoming the initial constructive expenses, increasing the unitary cost of water.

Comparing the two collectors it is possible to observe that in terms of water production the results are almost the same, meanwhile considering the SF the ETC technology obtains better results. Although, it is important to underline that the PSC's collecting area is 2.5 times less than the ETC ones, allowing the former to be more efficient in heat transfer, but with a higher technology cost than the ETC. Indeed, 24 m^2 of evacuated tubes cost $\sim 14,000$ € and one parabolic collector (9.583 m^2) cost $\sim 15,000$ €. This last difference strongly influences the water final price due to the fact that the collector represent the major expense of the plant (see Figures 4.3 and 4.8).

In conclusion the ETC collectors are more convenient than the PSC, even if the overall plant production is still not satisfactory.

4.2 Passive device

4.2.1 Numerical Analysis

Introduction

COMSOL Multiphysics is a finite-element based software, which allows to solve a consistent amount of issues, necessitating different physics. Indeed, the preliminary steps when initializing a simulation are the choice of: the spatial dimension (i.e 2D,1D or 3D) and the physics involved (i.e heat transfer or fluid flow). In this particular case three physics have been selected:

1. **Heat Transfer in Porous Media:** it allows to trace the different heat exchanges, considering also porous materials (i.e the hydrophilic membrane);

2. **Transport of Diluted Species:** it allows the evaluation of mass transport through the membranes, necessary to trace the fresh water mass flow;
3. **Laminar Flow:** used to fully determine the laminar flow of fluids, useful to describe the water flow in the hydrophilic layers by means of capillarity;

The biggest advantage of this software is the capability of linking the different physics during the solution of the problem. In particular, the heat transfer and the laminar flow effects have been considered simultaneously, elaborating a **non-isothermal fluid flow**. Once set this preliminary parameters the geometry can be directly generated thanks to the software's available geometry tools. The different parts of the model can be assigned to a material type and to a specific physical condition, so to prepare the software for the simulation. Lastly, a correct mesh can be generated and the simulation can be launched. Once ended, COMSOL Multiphysics has several post-processing tools to retrieve the required information from the model and solve the proposed problem.

In the following sections: the geometry, the physics, the boundary conditions involved and the obtained results will be deeply illustrated.

Geometry & Material characteristics

The 5-stages passive device has been assembled by stacking several rectangular boxes one on top of the other, with dimensions described in Section 3.3. The model geometry is shown in Figure 4.13.

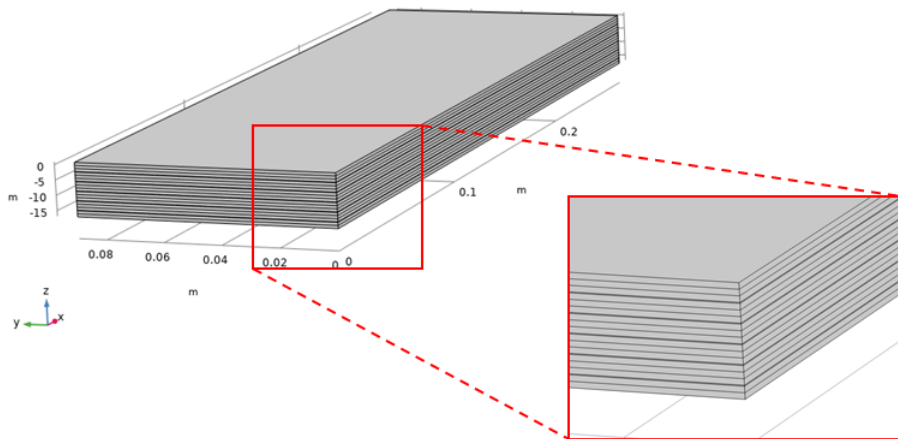


Figure 4.13: Geometry with detail

From the detail in figure, it is possible to observe that the middle 4 stages contain 5 boxes representing in series: aluminum foil, evaporator, membrane (thinner layer), condenser and second aluminum foil. The only exception is represented by the upper stage which

counts also an additional aluminum layer, working as solar absorber. As in real life, the hydrophilic and the aluminum layers are 1 mm thick and the membranes are 0.15 mm thick.

All the materials necessary for the simulation have been found in the software's material library, namely: aluminum, PTFE (membrane), microfiber (hydrophilic layer), water (hydrophilic layer) and air present in the membrane gaps. Since the materials are already available, the software is capable of retrieving all the important physical parameters necessary for the simulation.

Both the hydrophilic layers are modelled considering a 70 % of water and a 30 % of microfiber, since the layers are fully saturated. Considering this fact, the thermal conductivity of the whole body has been calculated as the weighted mean of the composing materials thermal conductivities:

$$k_{hydrophilic} = k_{microfiber} * 0.3 + k_{water} * 0.7 \quad (4.3)$$

where $k_{microfiber} = 0.04 [W/(mK)]$ and $k_{water} = 0.6 [W/(mK)]$.

The membrane instead contains micro pores filled with air, so the thermal conductivity of the whole layer is given by the parallel of the membrane's and the air's thermal conductivities. The searched parameter can be expressed as:

$$\frac{1}{k_{memlayer}} = \frac{1}{k_{air}\epsilon_m + (1 - \epsilon_m)k_{PTFE}} \quad (4.4)$$

where: ϵ_m is the membrane porosity, $k_{air} = 0.026 [W/(mK)]$ and $k_{PTFE} = 0.25 [W/(mK)]$. Due to the high porosity of the membrane, the overall thermal conductivity will be close to the air's one ($\sim 0.06 W/(mK)$).

Finally, the remaining aluminum layers are fully constituted by the base material, so can use the thermal conductivity present in the software's library.

Physics & Boundary conditions

The physics involved in the stationary simulation are illustrated in Section 4.2.1. Indeed, the main goal of the simulation is to predict the water vapour flux and the temperature profile of the device during operation, so the transient has a limited interest.

The heat transfer affects all the device, meanwhile the transport of the diluted species and the laminar flow are respectively restricted in the membranes and evaporators domains. The condenser's water flow has been omitted, since is nearly static ($Re \ll 1$) and its influence in the overall process is negligible .

As mentioned in Section 4.2.1 the water vapour flux has been evaluated separately from remaining the physics, allowing the software to solve the Navier-Stokes equations inde-

pendently. Always for this reason, the latent heat of evaporation transferred across the membrane has been modelled as a boundary condition present on the surface separating this last and the evaporator. In particular:

$$Q_{latent} = J \cdot \Delta H_v = \lambda \cdot \Delta H_v \quad (4.5)$$

where: ΔH_v is the latent heat of evaporation, J is the mass water vapour flux and λ is the lagrangian multiplier, necessary to solve the numerical solution by means of the "Lagrangian multiplier" approach.

COMSOL multyphysics is only capable of working with concentrations when dealing with mass transport, so in order to evaluate the molar flux across the membrane Equation 3.4 is written as follows:

$$N = -D_{eff} \nabla c = -D_{eff} \nabla \left(\frac{p_v}{RT} \right) \quad (4.6)$$

where: N [$mol/(m^2s)$] is the diffuse molar flux, D_{eff} the effective diffusion coefficient and c the molar concentration. In this specific case of study no air is present in between the evaporator and the membrane, so the contributions to the effective diffusion coefficient are given exclusively by Knudsen and molecular transport. Considering the theoretical assumptions illustrated in Section 3.4, D_{eff} can be evaluated as:

$$\frac{1}{D_{eff}} = \frac{1}{D_{wK}} + \frac{1}{D_{wa}} \quad (4.7)$$

where the former represents the Knudsen contribute, in particular:

$$D_{wK} = \frac{8r}{3} \sqrt{\frac{RT}{2\pi M_w}} \frac{\epsilon_m}{\tau} \quad (4.8)$$

and the latter represents the molecular contribute:

$$D_{wa} = 1.19 \cdot 10^{-4} \frac{T^{1.75}}{P} \frac{\epsilon_m}{\tau} \quad (4.9)$$

The initial molar concentration has been evaluated as:

$$c_0 = \frac{\phi_{rel} \rho_{max}}{M_w} \quad (4.10)$$

where: ϕ_{rel} is the relative humidity (0.2 in this case), ρ_{max} [kg/m^3] is the maximum water density with unitary relative humidity, namely $0.0172 \text{ kg}/m^3$.

In order to model the different heat transfers of the device with the environment, different boundary conditions have been imposed. The solar irradiance has been set as an incoming heat flux gathered by the solar absorber, which has an emissivity of 0.45 (Figure 4.14). As already said in Section 3.3, the constant value of irradiance has been set to $1000 \text{ W}/m^2$ basing on the machine's capacity.

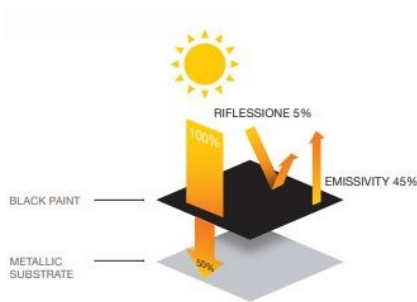


Figure 4.14: Black paint solar absorber emissivity [50]

Convective heat transfers occur on all the sides of the device, namely lateral, top and bottom. Due to the presence of the fans a forced convection has been considered for the top and bottom sides ($\sim 25 \text{ W}/(\text{m}^2\text{K})$), meanwhile thanks to the presence of the plastic envelopes the lateral heat loss has been considered limited ($\sim 3 \text{ W}/(\text{m}^2\text{K})$). Furthermore, considering the closed environment and the elevated amount of radiation, the ambient temperature has been considered ranging between 30-35 °C. Finally, the bottom radiation heat loss has

been considered, imposing the raw aluminum emissivity equal to 0.2.

The boundary conditions imposed to the laminar flow consist in the inlet and outlet flow conditions, attributed respectively to the lateral borders and the bottom side of the evaporators. The former consisted in assigning an inlet velocity to the fluid, namely $3.65 \times 10^{-6} \text{ m/s}$. This value has been obtained considering the distilled water production in the static case (no laminar flow). The former instead has been set by a pressure border condition which avoids water come back.

Mesh

In order to build the mesh two options have been selected: *Free Triangular* (for the sides where the fluid enters) and "Swept" (for the sides parallel to the fluid flow).

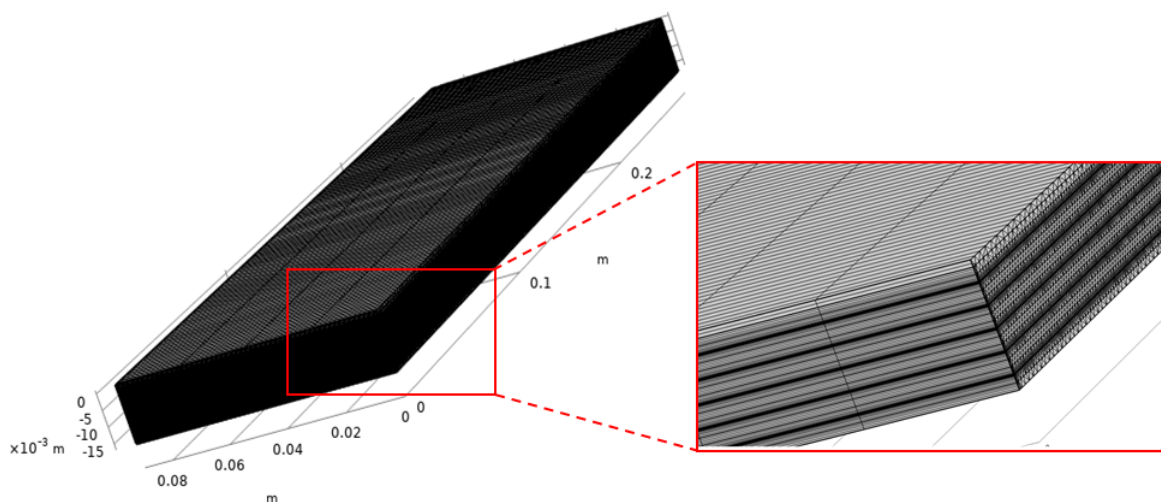


Figure 4.15: Detail view of meshed model

Given the big thickness difference between the membrane and the remaining blocks, the mesh on these borders had to be fined by a manual operation. The overall number of

elements built are 142604, with 322715 degrees of freedom plus 204538 internal degrees of freedom.

Results

Once ended the initial set-up, it is possible to run the simulation and elaborate the data by an aimed post-processing. Given the low complexity of the problem the simulation arrived to convergence in small time with only 3 iterations, as shown in Figure 4.16.

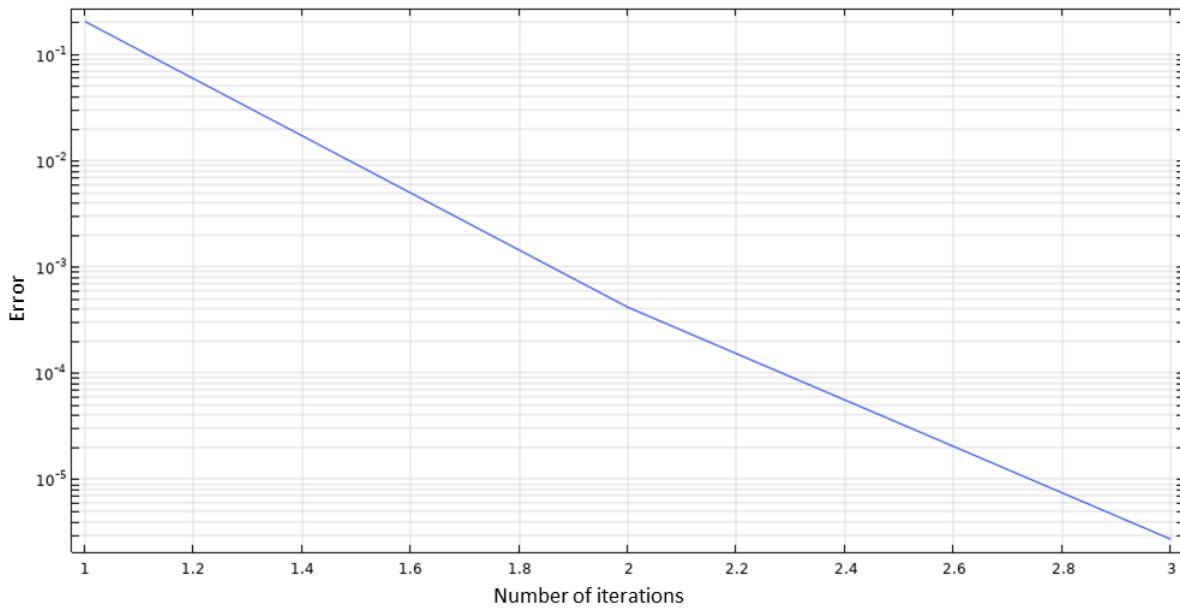


Figure 4.16: Error plot

The ambient temperature has been considered equal to 30 or 35 °C, meanwhile the convective heat transfer of the bottom and top has been considered equal to 25 or 30 $W/(m^2K)$, which are reasonable values for environment conditions. Combining these 4 values it is possible to obtain 3 different scenarios.

The most important value to consider is the fresh water production. In Table 4.5 are reported the latter data and the discrepancy with the experimental results, shown in Section 4.2.2.

The efficiencies related to the simulated cases are: $\eta_{1st} = 21.6\%$, $\eta_{2nd} = 20.7\%$ and $\eta_{3rd} = 19.5\%$, evaluated by means of the following equation:

$$\eta = \frac{N\Delta h_v}{q_{solar}} \quad (4.11)$$

The lower efficiency of this device respect to the older version [49] can be justified by the higher emissivity of the absorbant surface and the absence of the bottom heat sink.

	T_{amb} [°C]	h_{conv} [$W/(m^2K)$]	Diffuse molar flux [$mol/(m^2s)$]	Productivity [$l/(m^2h)$]	Difference [%]
1st case	35	30	0.025	1.62	8.89
2nd case	35	25	0.024	1.55	13.22
3rd case	30	25	0.023	1.46	18.14

Table 4.5: Simulation water production results

Once given the total water production of the device it is important to observe the performances of the single stages.



Figure 4.17: Diffuse water fluxes in the different stages

In Figure 4.17 it is possible to observe that the productivity is descendent from the top to the bottom of the device, coherently with the expected behaviour. The values are negative due to the opposite orientation of the axis respect to the water flux direction. The respective contribution of each stage, compared to the final productivity are: 21.96%, 20.99%, 19.98%, 19.01%, 18.05%.

It is now important to analyse the temperature profile along the device, since this last directly influences its productivity and the partial pressures present in the different layers (see Equation 3.1). For sake of simplicity the reported graphs refer to the second case of Table 4.5, which represents the most plausible situation. In Figure 4.18 is shown the volumetric temperature profile, meanwhile in Figure 4.19 is shown the temperature profile along the device's height.

Analysing Figure 4.18 it is possible to observe that the temperature ranges between 342 K (~ 69 °C), present on the solar absorber, and 328 K (~ 55 °C), on the bottom aluminum surface. Overall the temperature drop from top to bottom is of 14 °C, with a ΔT of 1 °C between evaporator and condenser of each stage. From Figure 4.19 it is possible to notice the different temperature drops when considering the material layers of the device.

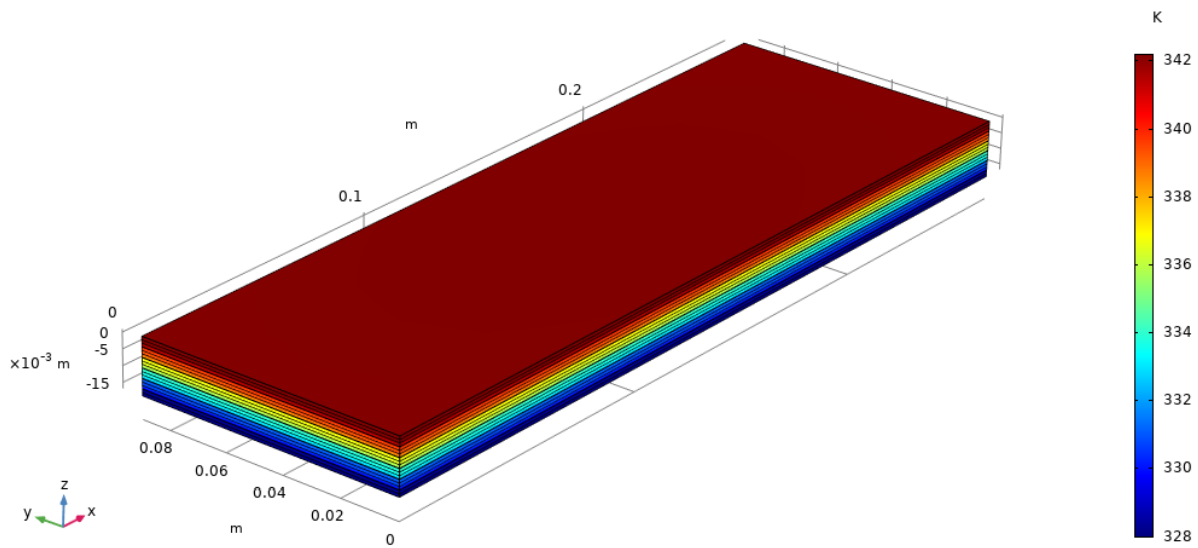


Figure 4.18: Volumetric temperature profile

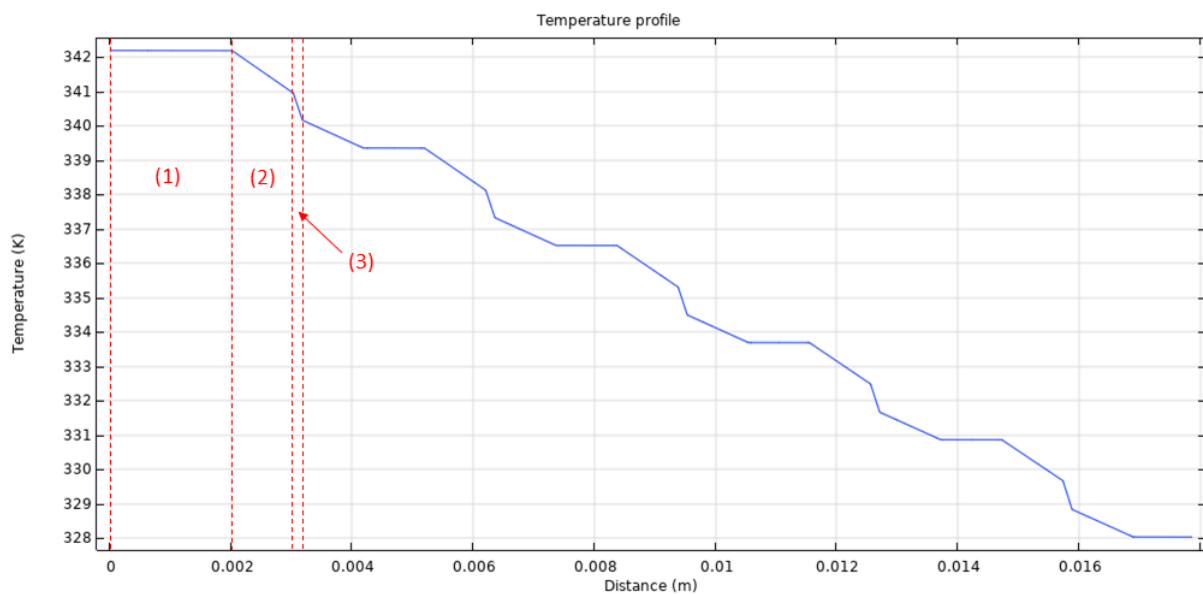


Figure 4.19: Temperature drop across the device's height. (1) corresponds to an aluminum substrate, (2) to an hydrophilic substrate and (3) to an hydrophobic substrate.

It is possible to inversely relate the slope of the curve with the thermal conductivity of the present material, namely higher the slope lower the thermal conductivity. Known this fact, zone (1) corresponds to an aluminum substrate, zone (2) to an hydrophilic substrate and zone (3) to an hydrophobic substrate. As previously mentioned, also this graph confirms the temperature drop of 1°C between the evaporator and the condenser of each stage.

Lastly is interesting to consider the distribution of the different lost heat fluxes. Table

4.6 illustrates the latter contributions.

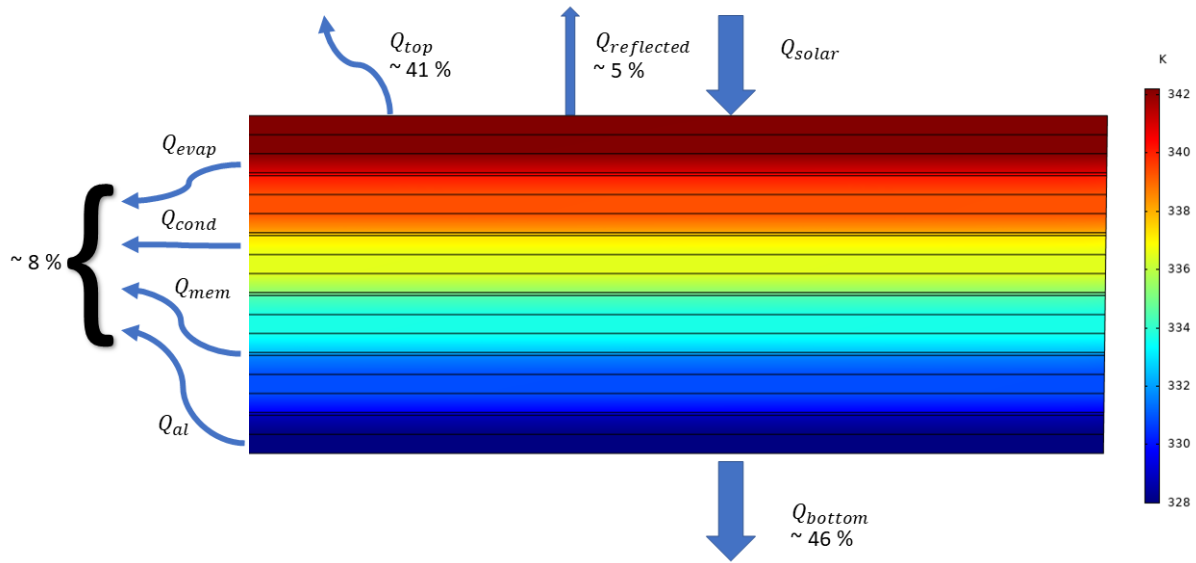


Figure 4.20: Section temperature distribution and thermal heat loss representation

Heat flux channel	Convective flux [mW]	Radiative flux [mW]	Total flux [mW]
Solar absorber	7896.7	2758.4	10655.1
Aluminum lateral	932.9	533.7	1466.6
Evaporator lateral	69.98	93.85	163.83
Condenser lateral	197.43	268.87	466.3
Membrane lateral	40.62	54.92	95.54
Bottom aluminum	11590	327.1	11917.1
Top reflected	/	/	1336

Table 4.6: Heat losses in the device

The top reflected lost heat has been evaluated considering the percentage reported in Figure 4.14. It is possible to relate these quantities to the total amount of solar irradiance incident on the solar absorber, namely 26.1 W . In Figure 4.20 are reported these values together with the temperature profile along the device's section.

4.2.2 Experimental results

The most important results retrieved by the experimental campaign carried out on the designed prototype are here reported. In particular, the best and the worst data sets are reported, outlining in particular the water production and the salinities registered on the evaporator.

Best Data Set

The data refer to the experiment taken under the sun simulator the 14/09/2020 with an irradiance of 1000 W/m^2 .

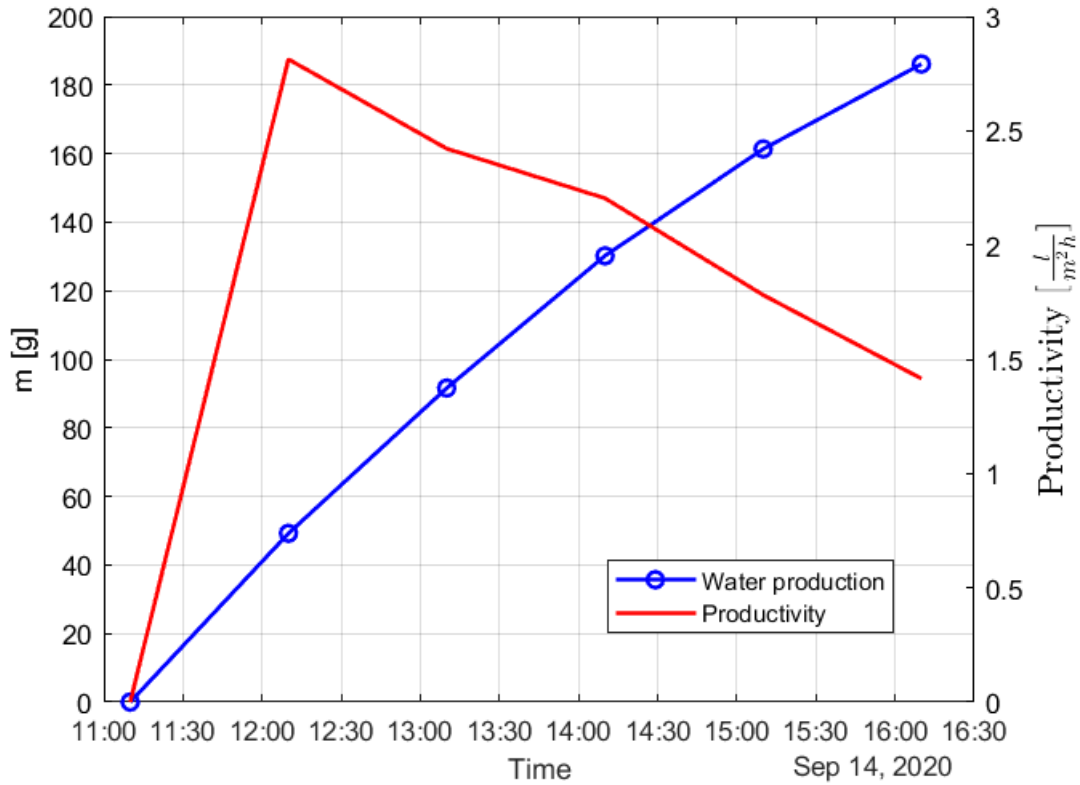


Figure 4.21: Distillate mass and productivity over time of a single device

[g/l]	Before test	After test	After 12 hours
Top Evaporator	35	161	35
Center Evaporator	35	112	35
Bottom Evaporator	35	54	35
Condenser	0	0	0
Distilled Water	/	0	0
Feed water	35	32	32

Table 4.7: Salinities on the first evaporator and condenser over time

From Figure 4.21 it is possible to observe that a total distilled mass of 186.12 grams and a mean productivity of $2.13 \text{ l}/(\text{m}^2\text{h})$ have been obtained over 5 hours. Table 4.8 confirms the capability of the device to recover the salinity of the evaporator during the hours of inactivity, which was one of the main goals of the new proposed geometry. Figure

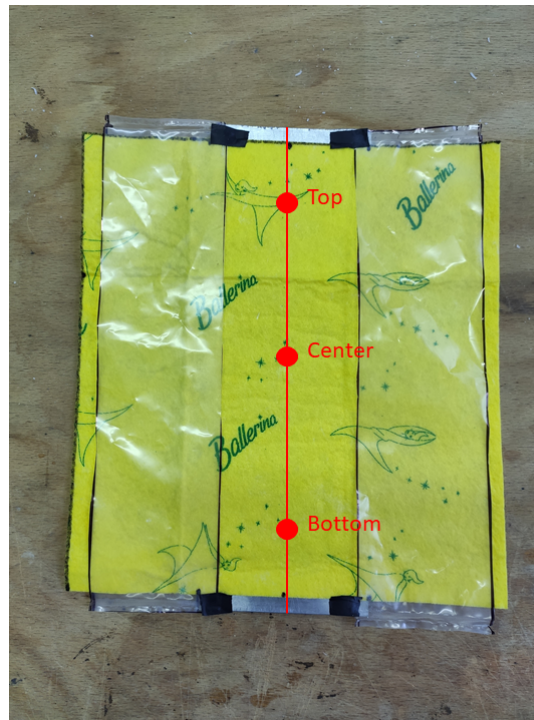


Figure 4.22: Evaporator's points for salinity measurement

4.22 allows to better understand the measurement points selected on the first evaporator, which represented the most critical situation.

Worst Data Set

The data refer to the experiment taken indoor the 18/09/2020 with an irradiance of 1000 W/m^2 .

[g/l]	Before test	After test	After 12 hours
Top Evaporator	35	125	35
Center Evaporator	35	112	35
Bottom Evaporator	35	88	35
Condenser	0	0	0
Distilled Water	/	0	0
Feed water	35	35	35

Table 4.8: Salinities on the first evaporator and condenser over time

From Figure 4.23 it is possible to observe that a total distilled mass of 125.5 grams and a mean productivity of $1.43 \text{ l}/(\text{m}^2\text{h})$ have been obtained over 5 hours. Also in this case Table 4.8 confirms the capability of the device to recover the salinity of the evaporator during the hours of inactivity.

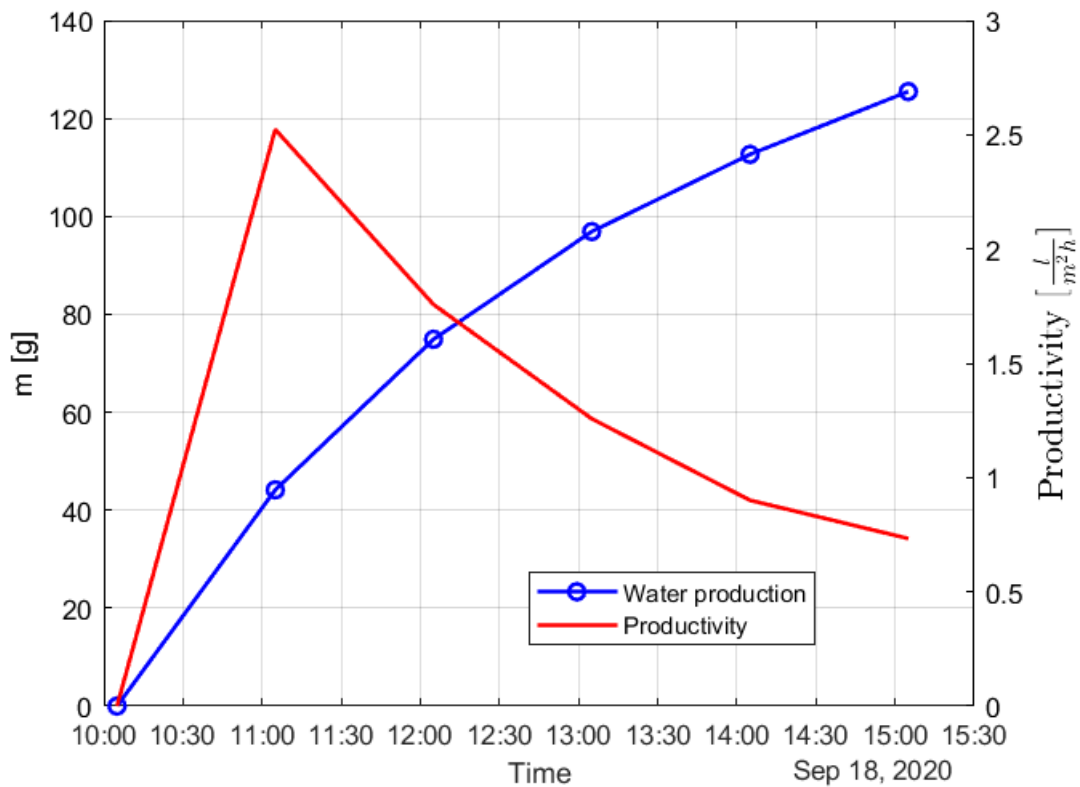


Figure 4.23: Distillate mass and productivity over time of a single device

4.2.3 Summary

Considering the experimental analysis, it has been obtained a mean distillate productivity of $1.78 l/(m^2h)$. As shown in Table 4.5 it is observable that the maximum percentual deviation respect to the mean experimental result is lower than 20 %, confirming the wellness of this latter data. Figure 4.24 visually represents this result by showing that the numerical model results interval is almost fully contained in the experimental one.

Considering a constant irradiance of $1000 W/m^2$ the productivity can be expressed as liters per kilowatts per hour incident on the absorbent surface, obtaining $1.78 l/kWh$. Considering the average solar irradiation of Muscat in September (i.e. 199 kWh per square meter per month, source: PVGIS) and the validated model estimates, the whole desalination technology would be able in average to produce 8.38 L/day of distilled water from seawater (6.74 L/day worst scenario; 10.03 L/day best scenario), largely full-filling the required water production required by the contest.

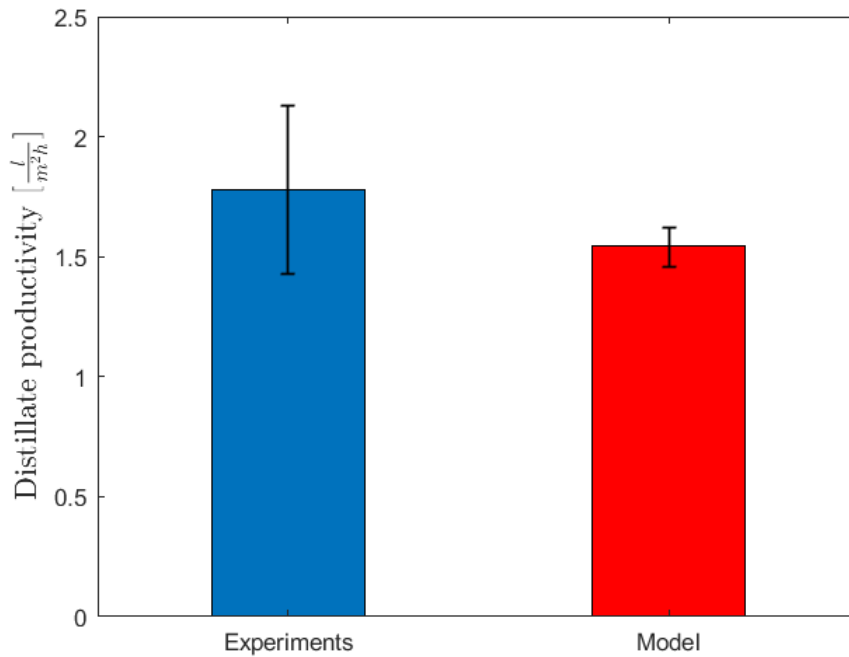


Figure 4.24: Distillate productivity comparison

4.3 Comparison of desalination performance

The main features analyzed are: distillate productivity, energy consumption, annual fresh-water production and cost per liter. Table 4.9 collects all these data regarding the 2 different technologies, where the productivity is referred to the membrane's dimension.

	Single Passive Device	Renewable Driven Active Plant	Literature Renewable Driven Active Plant [51]
Productivity [$l/(m^2h)$]	1.78	4.86	/
Power consumption [kWh/m^3]	562	3238	/
Annual water production [$l/year$]	85	8523	36500
Freshwater cost [$€/l$]	0.0472	0.31	0.015

Table 4.9: Comparison between the two technologies

These results consider a single passive device (contained in a panel), the fourth configuration of the plant adopting ETC collectors and a solar powered MD plant with $10 m^2$ membrane found in literature. It is noticeable the higher annual water production and productivity of the active system, although obtainable by means of a ~ 5 times higher energy consumption. Indeed, the water cost of this latter is ~ 7 times higher than the passive's one. Furthermore, it is important to consider the modularity of the passive de-

vice which could allow the whole apparatus to reach these levels of production by simply adding more devices.

The active system is capable of providing a constant amount of water along the year thanks to the presence of the auxiliary system, meanwhile the passive device depends exclusively on the solar irradiance, varying the production during the different seasons. This higher reliability is fundamental when a certain daily amount of water is necessary (i.e for agriculture or biological issues). It is also important to underline that the results reported for the passive device have been obtained in favorable conditions and longer experimental campaigns must be done in order to analyse the behaviour along the different climatic conditions.

Nevertheless basing on this results it is possible to conclude that the Membrane Distillation desalination method applied to passive devices generates satisfying results, which can be compared to the more used active technology.

5. Conclusions and Future Works

Water scarcity is a more and more striking problem for the global populations. To face this problem, the researchers all over the world are developing new methods to retrieve freshwater, mainly based on seawater (or saltwater) desalination in order to minimize the depletion of the groundwater resources. Membrane Distillation is of particular interest due to the possibility of improvement, especially considering: the lower pressure and temperature levels required for the process respect to other technologies, the easy coupling of the plant with renewable energy sources, the low maintenance and the low complexity. The main objectives of this thesis were to study this desalination technique implemented in an scaled active plant and study the possibility of using it in a new low cost passive device, both adopting solar irradiation as main energy source. The Simulink model describing the former is capable of predicting the water production of the plant, allowing to precisely evaluate its performances considering existing components acquirable from the different manufacturers. While established active technologies MD based are already present in the literature, passive ones are still under development, this is why a new prototype has been presented and compared to the existing technologies, so to evaluate its capabilities and eventual large scale production. Generally speaking passive desalination reduces the energy consumption of the process and eliminate the environmental issue linked with the brine production typical of active plants, yielding in contrast lower water productions. These devices are ideal to be employed in remote areas and to diversify the global freshwater production.

Mainly due to the limited dimensions of the plant, in particular of the membrane used, in order to hold an acceptable solar fraction the annual water production has been limited if compared to the other plants present in literature (adopting 10 m^2 membranes or working with fuel combustion). Despite this fact, important information regarding these last parameters and the energy consumption have been retrieved, namely in the optimal configuration it has been found: a solar fraction of 50 %, an annual water production of 8523 l/year , a specific power consumption of 3238 kWh/m^3 considering both solar irradiation and fuel consumption and lastly a specific water cost of 0.31 €/l . Furthermore, a more efficient collector type, namely the Parabolic Solar Collector (PSC) has been tested providing a higher heat transfer capacity per meter squared, yielding though to a higher

investment increasing the unitary water cost. The obtained results are more than sufficient to fully characterize the plant and to provide reliable data comparable with the analogous passive technology, therefore the further optimization is left as a future work (i.e use of a stratified tank, variation of collectors and membrane's dimension and coupling with different desalination technologies).

The design of the passive device has been carried out following the guidelines imposed by the the OHDC (Oman Humanitarian Desalination Challenge) desalination challenge. All the requests, namely: low cost, easy handling, short term use, robustness, minimum rate of production and water quality, have been fully satisfied by the proposed prototype. After the initial design process, the performances of the device have been obtained by both successful experiments and numerical simulations. Considering a constant solar irradiation of 1000 W/m^2 the device has been capable of showing: a mean productivity of $1.78 \text{ l/(m}^2\text{h)}$, an annual water production of 85 l/year , a specific power consumption of 562 kWh/m^3 and a specific water cost of 0.0472 €/l . Considering the low cost and simplicity of construction, comparing them with the ones retrieved with the already consolidated active technology and considering that the device has been productive only 5 hours per day, the results achieved are promising. From the numerical calculations it has been possible to observe that the passive device has a lower energy consumption, lower cost and lower water production respect to the other desalination technology. This latter though is easy to overcome simply increasing the number of devices composing the apparatus, i.e considering 20 devices as for the OHDC competition it is possible to achieve 1700 l/year . The innovative symmetrical geometry demonstrated to allow a complete salt removal during the simulated nighttime, thus enhancing the low operational maintenance required by the apparatus compared to the previous versions. Furthermore, the numerical simulations performed with COMSOL Multiphysics have been capable of predicting the behaviour of the device and confirming the experimental results. As future work, it would be interesting to execute an outdoor experimental campaign and evaluate the device's productions under daily variable solar irradiations.

In conclusion, it is possible to assert that the Membrane Distillation technology can be fully implemented in passive devices, obtaining satisfying energetic and productive results opening a new perspective for desalination.

5. Bibliography

- [1] *Water Scarcity*. URL: <https://www.worldwildlife.org/threats/water-scarcity>. (accessed 11.09.2020).
- [2] WWAP(World Water Assessment Programme). “The United Nations World Water Development Report 4: Managing Water under Uncertainty and Risk”. In: Scientific and Cultural Organization (2012).
- [3] Abd El-Kodous Mohamed. “C-dots dispersed macroporous TiO₂ nanospheres as an efficient photocatalyst for waste-water treatment”. In: (2018). DOI: [10.13140/RG.2.2.25280.38404](https://doi.org/10.13140/RG.2.2.25280.38404).
- [4] Food and Agriculture Organization of the United Nations. “Review of the World Water Resources by Country”. In: volume 23 (2012).
- [5] Sammy Roth. “California’s last resort: Drink the Pacific”. In: Desert Sun (2015).
- [6] Simon Gottelier. “A desalination boom in California could help it deal with exceptional droughts”. In: The Guardian (2014).
- [7] Mohammad Ali Abdelkareem et al. “Recent progress in the use of renewable energy sources to power water desalination plants”. In: *Desalination* 435 (2018), pp. 97–113. URL: <http://www.sciencedirect.com/science/article/pii/S0011916417321306>.
- [8] Manish Thimmaraju Divya Sreepada Gummadi Sridhar Babu Bharath Kumar Dasari Sai Kiran Velpula and Nagaraju Vallepu. “Desalination of Water”. In: (2018). DOI: [10.5772/intechopen.78659](https://doi.org/10.5772/intechopen.78659).
- [9] Pei Xu Tzahi Y. Cath Alexander P. Robertson Martin Reinhard James O. Leckie and Jörg E. Drewes. *Critical review of desalination concentrate management, treatment and beneficial use*. Environmental Engineering Science. 2013.
- [10] Manjula Nair and Dinesh Kumar. “Water desalination and challenges: the middle-east perspective: a review”. In: Desalination and Water Treatment (2013).
- [11] *What is Reverse Osmosis?* URL: <https://puretecwater.com/reverse-osmosis/what-is-reverse-osmosis>. (accessed 15.09.2020).

- [12] S. Jamaly NN, Darwish I, Ahmed and SW, Hasan. *A short review on reverse osmosis pretreatment technologies*. Desalination. 2014.
- [13] RM, Garaud SV, Kore VS, Kore and GS, Kulkarni. "A short review on process and applications of reverse osmosis". In: *Universal Journal of Environmental Research & Technology* (2011).
- [14] Muhammad Wakil Shazad Muhammad Burhan and Kim Choon NG. "Pushing desalination recovery to the maximum limit: Membrane and thermal processes integration". In: *Desalination* (2017).
- [15] Mark Wilf and Craig Bartels. "Optimization of seawater ro systems design". In: *Desalination* (2005).
- [16] Siobhan Boerlage and Nabil Nada. "Algal toxin removal in seawater desalination processes". In: *Desalination and Water Treatment* 55 (Sept. 2014), pp. 1–19. DOI: [10.1080/19443994.2014.947785](https://doi.org/10.1080/19443994.2014.947785).
- [17] Dhananjay Mishra. "Desalination for cost-effective water production". In: *Advisian Worley Group* (2017).
- [18] Junjie Zhao Minghui Wang Haitham MS Lababidi Hamad Al-Adwani and Karen K Gleason. "A review of heterogeneous nucleation of calcium carbonate and control strategies for scale formation in multi-stage flash (msf) desalination plants". In: *Desalination* (2018).
- [19] Ali Al-Karaghoul and Lawrence L. Kazmerski. "Energy consumption and water production cost of conventional and renewable-energy-powered desalination processes". In: *Renewable and Sustainable Energy Reviews* 24 (2013), pp. 343–356. ISSN: 1364-0321. DOI: <https://doi.org/10.1016/j.rser.2012.12.064>. URL: <http://www.sciencedirect.com/science/article/pii/S1364032113000208>.
- [20] Noredine Ghaffour Thomas M Missimer and Gary L Amy. "Technical review and evaluation of the economics of water desalination: current and future challenges for better water supply sustainability". In: *Desalination* (2013).
- [21] Chennan Li Yogi Goswami and Elias Stefanakos. "Solar assisted sea water desalination: a review". In: *Renewable and Sustainable Energy Reviews* (2013).
- [22] Abdulaziz M. Alkhalifa and Noam Lior. "Membrane-distillation desalination: status and potential". In: *Desalination* (2005).
- [23] Emis. "Membrane Distillation". In: (). URL: <https://emis.vito.be/en/bat/tools-overview/sheets/membrane-distillation>.

- [24] Ruh Ullah Majeda Khraishah Richard J Esteves James T McLeskey Jr Mohammad AlGhouti Mohamed Gad-el Hak and H Vahedi Tafreshi. “Energy efficiency of direct contact membrane distillation”. In: *Desalination* (2018).
- [25] S.W. Sharshir et al. “Factors affecting solar stills productivity and improvement techniques: A detailed review”. In: *Applied Thermal Engineering* 100 (2016), pp. 267–284. ISSN: 1359-4311. DOI: <https://doi.org/10.1016/j.applthermaleng.2015.11.041>. URL: <http://www.sciencedirect.com/science/article/pii/S1359431115012879>.
- [26] Vishwanath Panangipalli et al. “Solar stills system design: A review. Renew. Sustain”. In: *Energy Rev* 51 (Jan. 2015), pp. 153–181.
- [27] George M. Ayoub and Lilian Malaeb. “Developments in solar still desalination systems: A critical review”. In: *Critical reviews in environmental science and technology* (2012).
- [28] Amimul Ahsan M. Imteaz Ukwuani A. Thomas MAzmi Aatur Rahman and NN. Nik Daud. “Parameters affecting the performance of a low cost solar still”. In: *Applied Energy* (2014).
- [29] Chao Chang et al. “Three-Dimensional Porous Solar-Driven Interfacial Evaporator for High-Efficiency Steam Generation under Low Solar Flux”. In: *ACS Omega* 4 (Feb. 2019), pp. 3546–3555. DOI: [10.1021/acsomega.8b03573](https://doi.org/10.1021/acsomega.8b03573).
- [30] European Commission. *Photovoltaic Geographical Information System*. URL: https://re.jrc.ec.europa.eu/pvg_tools/it/#MR. (accessed 25/09/2020).
- [31] L.T. Wong and W.K. Chow. “Solar radiation model”. In: *Applied Energy* 69.3 (2001).
- [32] John A. Duffie and William A. Beckman. *Solar Engineering of Thermal Processes*. 2013.
- [33] Amir Farzaneh. *InTech-Aluminium alloys in solar power benefits and limitations*. Aug. 2016.
- [34] MicroPowers. *Dish type Stirling solar thermal power generation technology*. URL: <http://www.micropowers.com/en/Dishstirling.aspx?cid=418>.
- [35] Vaillant. *auroTHERM exclusive*. URL: <https://www.vaillant.it/home/prodotti/aurotherm-exclusive-1986.html>.
- [36] Matteo Morciano et al. “Installation of a Concentrated Solar Power System for the Thermal Needs of Buildings or Industrial Processes”. In: *Energy Procedia* 101 (2016). ATI 2016 - 71st Conference of the Italian Thermal Machines Engineering Association, pp. 956–963. ISSN: 1876-6102. DOI: <https://doi.org/10.1016/j.egypro.2016.11.121>. URL: <http://www.sciencedirect.com/science/article/pii/S1876610216313303>.

- [37] Marco F. Torchio. *Tabelle di termodinamica Applicata e Trasmissione del Calore*. Ed. by CLUT. 2012.
- [38] Marco F. Torchio. *Tabelle di termodinamica Applicata e Trasmissione del Calore*. Ed. by CLUT. 2012.
- [39] *Brazed plate heat exchangers - Examples of application*. URL: <https://www.brazed-plate-heat-exchanger.com/anwendungen.htm>. (accessed 20/07/2020).
- [40] Vaillant. *aguaFLOW*. URL: <https://www.vaillant.it/home/prodotti/aguaflow-11072.html>. (accessed 15.07.2020).
- [41] L. Eykens et al. “Characterization and performance evaluation of commercially available hydrophobic membranes for direct contact membrane distillation”. In: *Desalination* 392 (2016), pp. 63–73. ISSN: 0011-9164. DOI: <https://doi.org/10.1016/j.desal.2016.04.006>. URL: <http://www.sciencedirect.com/science/article/pii/S001191641630159X>.
- [42] Francesco Artuso. *Solar Concentration and Membrane Distillation coupling: System Model and Case Studies*.
- [43] Matteo Morciano Matteo Fasano Matteo Alberghini Eliodoro Chiavazzo Pietro Asinari. “Passive solar high-yield seawater desalination by multi-stage low-cost distillation for humanitarian crises”. In: OHDC (2019).
- [44] Paul Reig Rutger Willem Hofste and Leah Schleifer. “17 Countries, Home to One-Quarter of the World’s Population, Face Extremely High Water Stress”. In: (2019). URL: <https://www.wri.org/blog/2019/08/17-countries-home-one-quarter-world-population-face-extremely-high-water-stress>.
- [45] *Oman Humanitarian Desalination Challenge*. URL: <https://desalinationchallenge.com/>. (accessed 02.10.2020).
- [46] World Health Organization. “Fourth Edition. Guidelines for drinking-water quality”. In: WHO chronicle (2017), 38(4):104–8.
- [47] “Solar passive distiller with high productivity and Marangoni effect-driven salt rejection”. In: *Energy & Environmental Science* (2020).
- [48] Bruce E Poling John M Prausnitz John P O’Connell. *The properties of gases and liquids*. Vol. 5. Mcgraw Hill New York, 2001.
- [49] Eliodoro Chiavazzo Matteo Morciano Francesca Viglino Matteo Fasano and Pietro Asinari. “Passive solar high-yield seawater desalination by modular and low-cost distillation”. In: *Nature Sustainability* (2018).

-
- [50] Almeco Group. *Tinox Energy*. URL: https://www.almecogroup.com/uploads/generic_file/1172-almeco_tinoxenergy_eng_s402_07_2014_mail_1_3.pdf.
- [51] Fawzi Banat and Nesreen Jwaied. “Economic evaluation of desalination by small-scale autonomous solar-powered membrane distillation units”. In: *Desalination* 220.1 (2008). European Desalination Society and Center for Research and Technology Hellas (CERTH), Sani Resort 22 –25 April 2007, Halkidiki, Greece, pp. 566–573. ISSN: 0011-9164. DOI: <https://doi.org/10.1016/j.desal.2007.01.057>. URL: <http://www.sciencedirect.com/science/article/pii/S0011916407006571>.